

# The CT18 QCD analysis with the LHC experimental data

**Pavel Nadolsky**

Southern Methodist University

**CTEQ-TEA (Tung et al.) working group**

**China Northeastern University:** T.-J. Hou

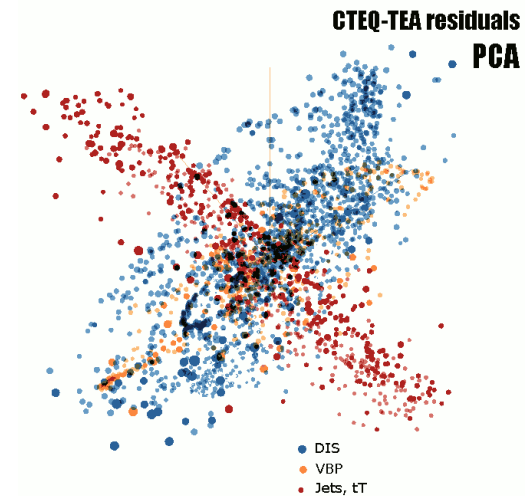
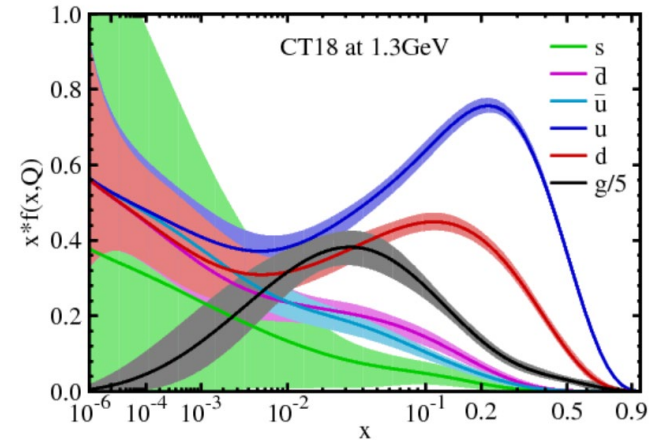
**Kennesaw State University:** M. Guzzi

**Michigan State U.:** J. Huston, J. Pumplin, D. Stump, C. Schmidt, J. Winter, C.-P. Yuan

**Shanghai Jiao Tong University:** J. Gao

**Southern Methodist University:** T. Hobbs, P.N., B.T.Wang, K. Xie

**Xinjiang University:** S. Dulat, I. Sitiwaldi



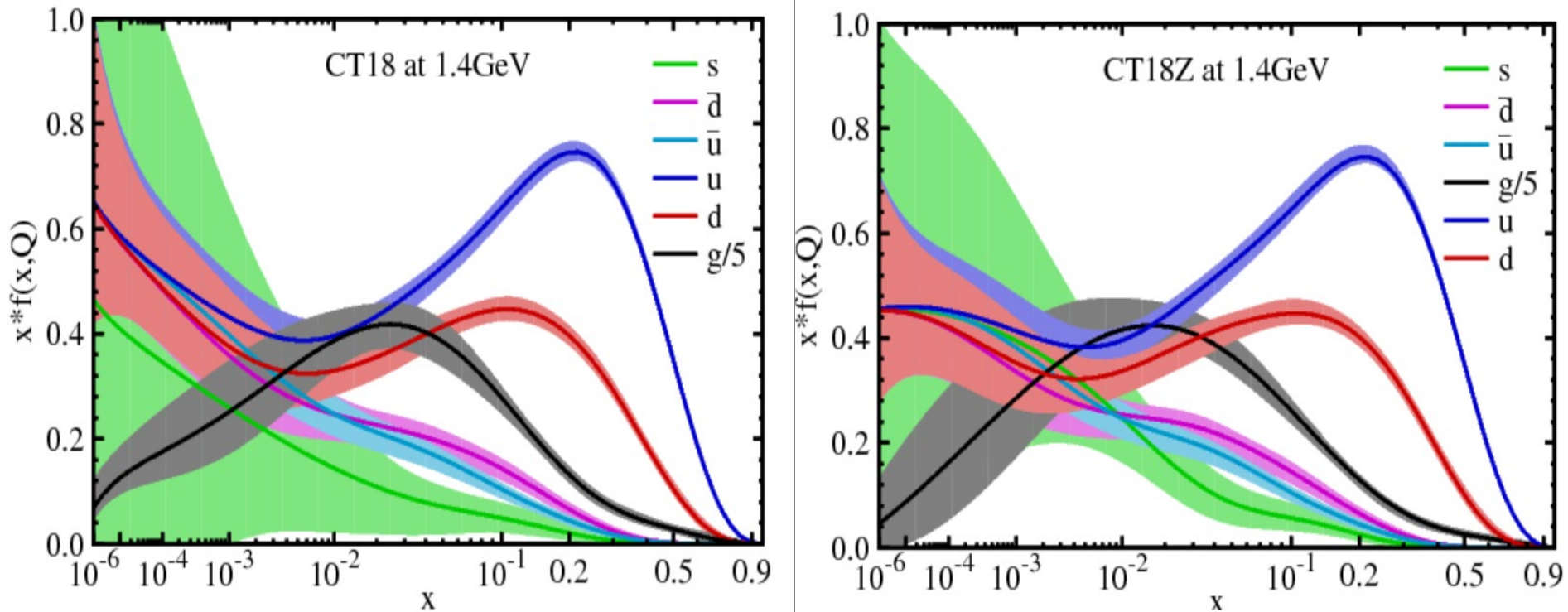
# Frontiers of the PDF analysis



Significant advances on all frontiers will be necessary to meet the targets of the HL-LHC program

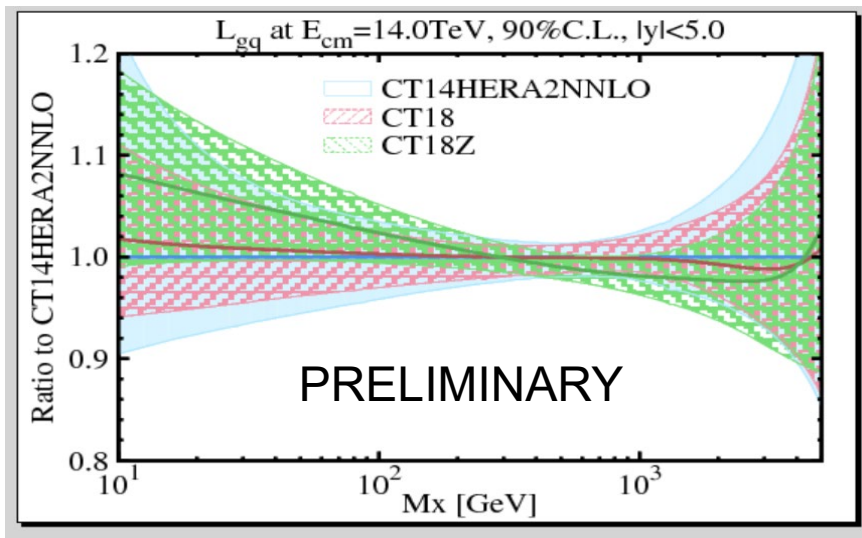
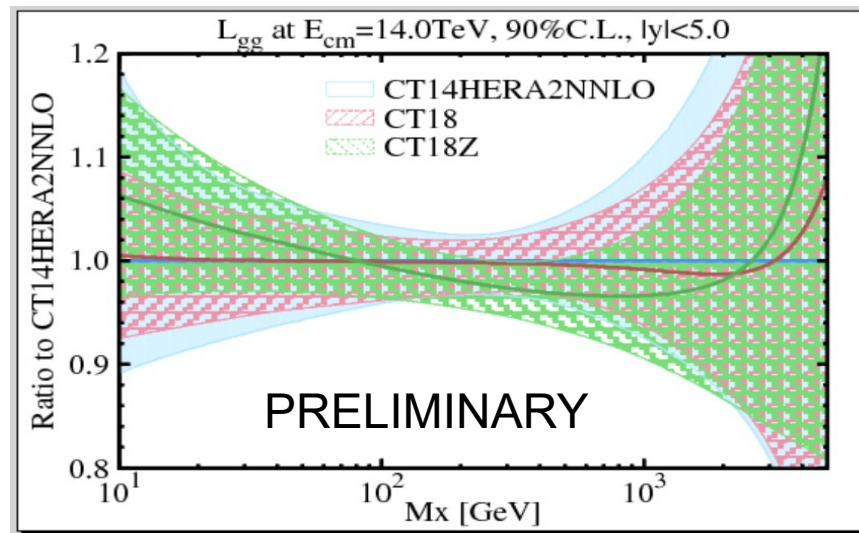
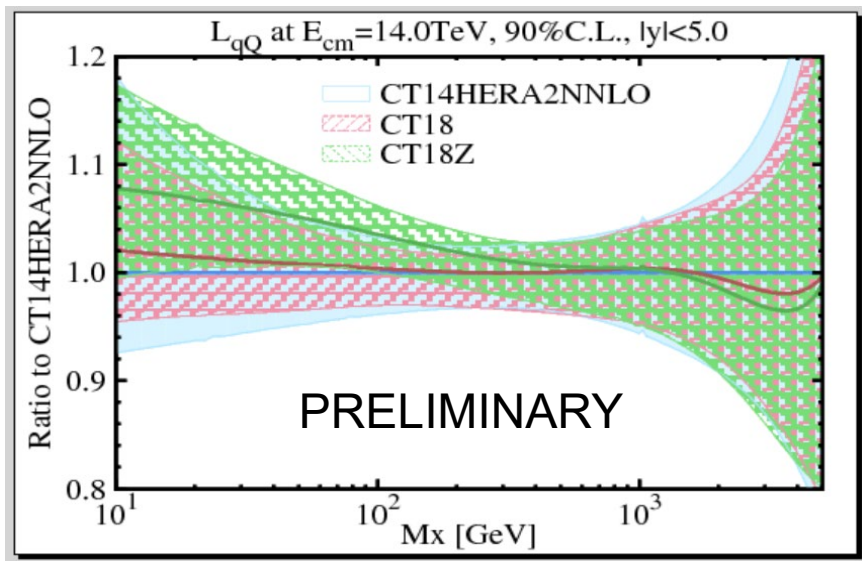
# CT18 parton distributions

Four PDF ensembles: CT18 (default), A, X, and Z



CT18Z has enhanced gluon and strange PDFs at  $x \sim 10^{-4}$ , and reduced light-quark PDFs at  $x < 10^{-2}$ . The CT18Z fit is performed so as to maximize the differences from CT18 PDFs, while preserving about the same goodness-of-fit as for CT18. CT18A and CT18X include some features of CT18Z

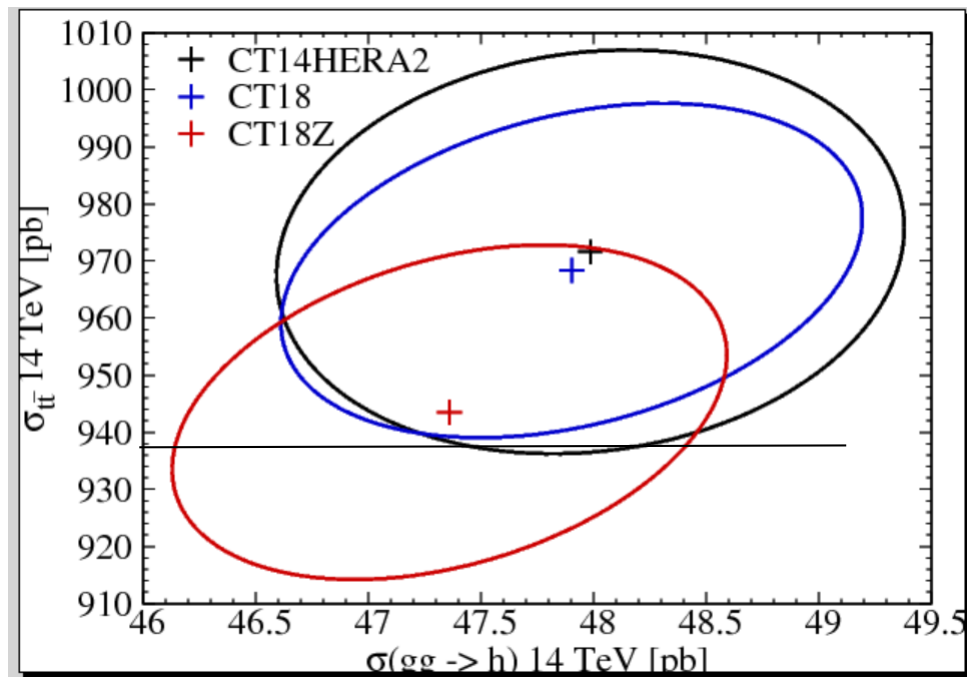
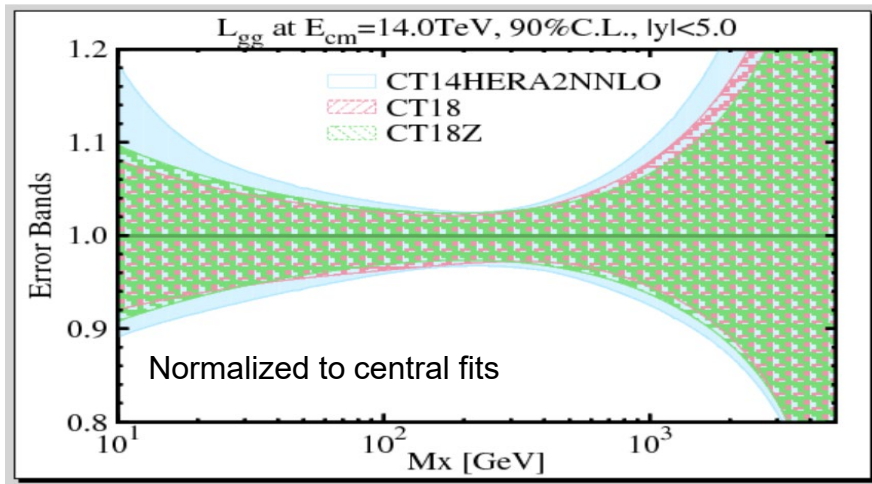
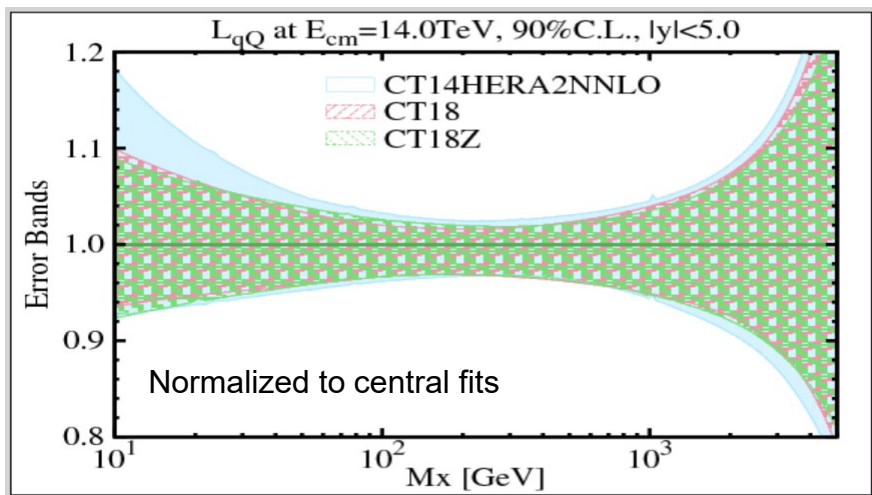
# CT18/CT18Z parton luminosities



CT18 consistent with CT14

CT18Z has a somewhat different shape, especially at low invariant masses  $M_X$

# Mild reduction in nominal PDF error bands and cross section uncertainties



CT18Z  $gg \rightarrow H$  and  $t\bar{t}$  production cross sections lower by about 1 and 2.5% compared to CT14HERA2

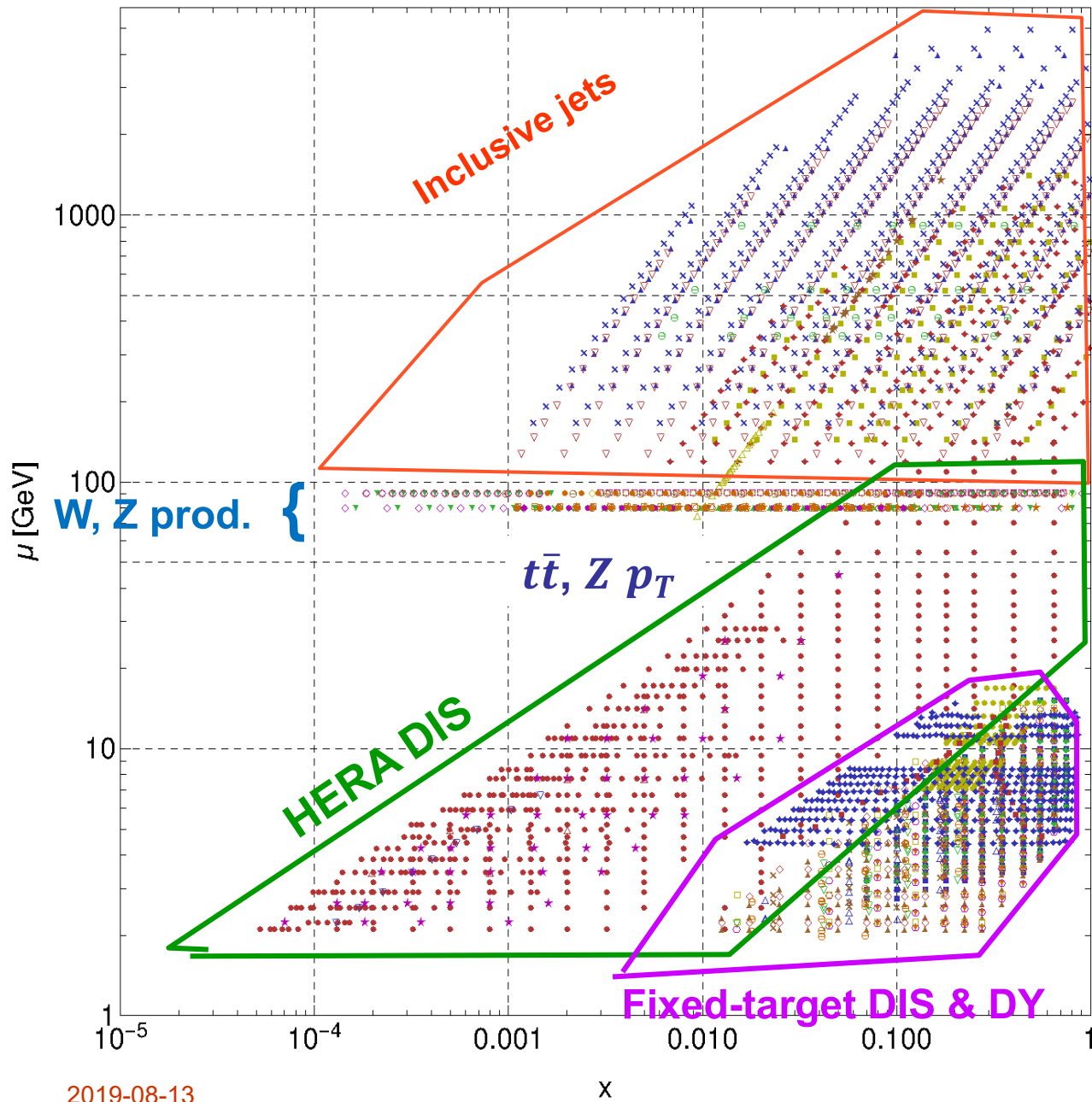
PRELIMINARY



# CT18 in a nutshell

- Start with CT14-HERA2 (HERAI+II combined data released after publication of CT14)
- Examine a wide range of PDF parameterizations
- Use as much relevant LHC data as possible using applgrid/fastNLO interfaces to data sets, with NNLO/NLO K-factors, or fastNNLO tables in the case of top pair production. **Benchmark the predictions!**
- Examine **QCD scale dependence** in key processes
- Implement **parallelization** of the global PDF fitting to allow for faster turn-around time
- Validate the results using a **strong set of goodness-of-fit tests** (*Kovarik, PN, Soper, arXiv:1905.06957*)
- Use diverse statistical techniques (**PDFSense, ePump, Gaussian variables, Lagrange Multiplier scans**) to examine agreement between experiments

# Experimental data in CT18 PDF analysis



- |                  |                         |
|------------------|-------------------------|
| ● HERA I+II'15   | ◇ ZYCDF2'10             |
| ■ BCDMSp'89      | △ HERAB'06              |
| ◆ BCDMSd'90      | ▽ HERA-FL'11            |
| ▲ NMCrat97       | × CMS7EASY'12           |
| ▼ CDHSW-F2'91    | ⊖ ATL7WZ'12             |
| ○ CDHSW-F3'91    | ★ D02EASY2'15           |
| □ CCFR-F2'01     | ● CMS7MASY2'14          |
| ◇ CCFR-F3'97     | ■ CDF2JETS'09           |
| △ NuTeV-NU'06    | ◆ D02JETS'08            |
| ▽ NuTeV-NUB'06   | ▲ ATLAS7JETS'15         |
| × CCFR SI NU'01  | ▼ LHCb7ZWRAP'15         |
| ⊖ CCFR SI NUB'01 | ○ LHCb8ZEE'15           |
| ★ HERAC'13       | □ CMS8WASY'16           |
| ● E605'91        | ◇ LHCb8WZ'16            |
| ■ E866RAT'01     | △ ATLASZPT'16           |
| ◆ E866PP'03      | ▽ CMS7JETS'14           |
| ▲ CDF1WASY'96    | × CMS8JETS'17           |
| ▼ CDF2WASY'05    | ⊖ CMS8TTB-PTTYT'17      |
| ○ D02MASY'08     | ★ ATLAS TTB-P TT-MTT'15 |
| □ ZYD02'08       | ● ATLAS7ZW'16           |

2019-08-13

# New LHC datasets for CT18

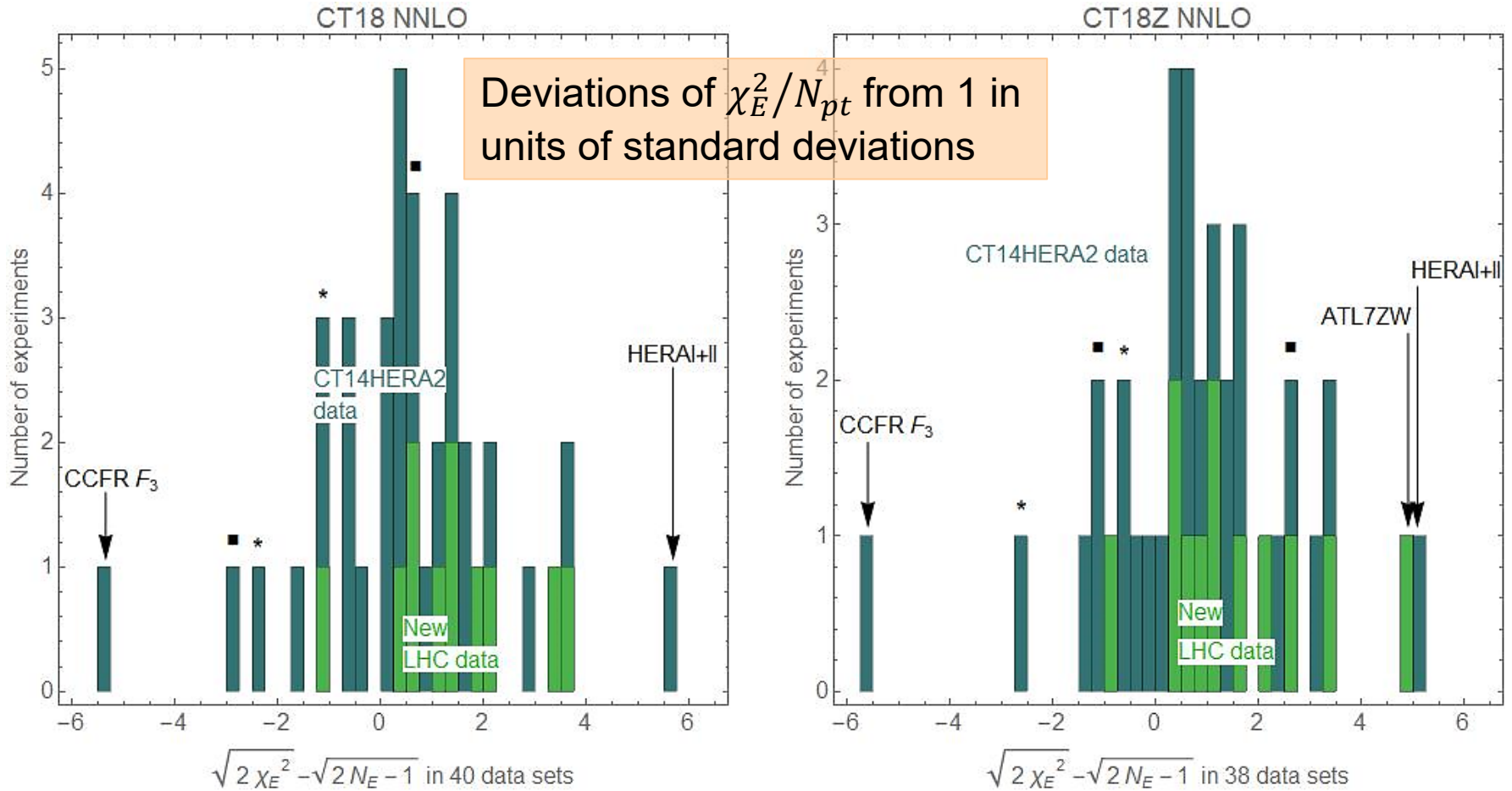
1. 245 1505.07024 LHCb Z (W) muon rapidity at 7 TeV(applgrid)
2. 246 1503.00963 LHCb 8 TeV Z rapidity (applgrid);
3. 249 1603.01803 CMS W lepton asymmetry at 8 TeV (applgrid)
4. 250 1511.08039 LHCb Z (W) muon rapidity at 8 TeV(applgrid)
5. 253 1512.02192 ATLAS 7 TeV Z pT (applgrid)
6. 542 1406.0324 CMS incl. jet at 7 TeV with R=0.7 (fastNLO)
7. 544 1410.8857 ATLAS incl. jet at 7 TeV with R=0.6 (applgrid)
8. 545 1609.05331 CMS incl. jet at 8 TeV with R=0.7 (fastNLO)
9. 565 1511.04716 ATLAS 8 TeV tT pT diff. distributions (fastNNLO)
10. 567 1511.04716 ATLAS 8 TeV tT mtT diff. distributions (fastNNLO)
11. 573 1703.01630 CMS 8 TeV tT (pT , yt ) double diff. distributions (fastNNLO)
12. 248 1612.03016 ATLAS 7 TeV Z and W rapidity (applgrid)->CT18Z
  - also uses a special small-x factorization scale, charm mass  $m_c=1.4$  GeV
  - serious changes in PDFs, so warrants a separate PDF



# CT18 (CT18Z) NNLO

13 (14) new LHC experiments with  
665 (711) data points

LHC experiments, especially ATLAS 7 TeV  $Z, W$  production (only in the CT18A and Z fits) tend to have elevated  $\chi_n^2/N_{pt}$  in global fits



# CT14 PDFs with HERA1+2 (=HERA2) combination

Phys.Rev. D95  
(2017) 034003

Separate the four HERA2 DIS processes;  
( $Q_{\text{cut}} = 2 \text{ GeV}$ )

	$N_{\text{pts}}$	$\chi^2_{\text{red.}} / N_{\text{pts}}$
NC $e^+p$	880	1.11
CC $e^+p$	39	1.10
NC $e^-p$	159	1.45
CC $e^-p$	42	1.52
totals		
[reduced $\chi^2$ ] / N	1120	1.17
$\chi^2 / N$	1120	1.25
$R^2 / N$	1120	0.08

$e^+p$  data are fitted fine

$e^-p$  data are fitted poorly

← reduced  $\chi^2$  values

←  $\chi^2 = [\text{reduced } \chi^2] + R^2$

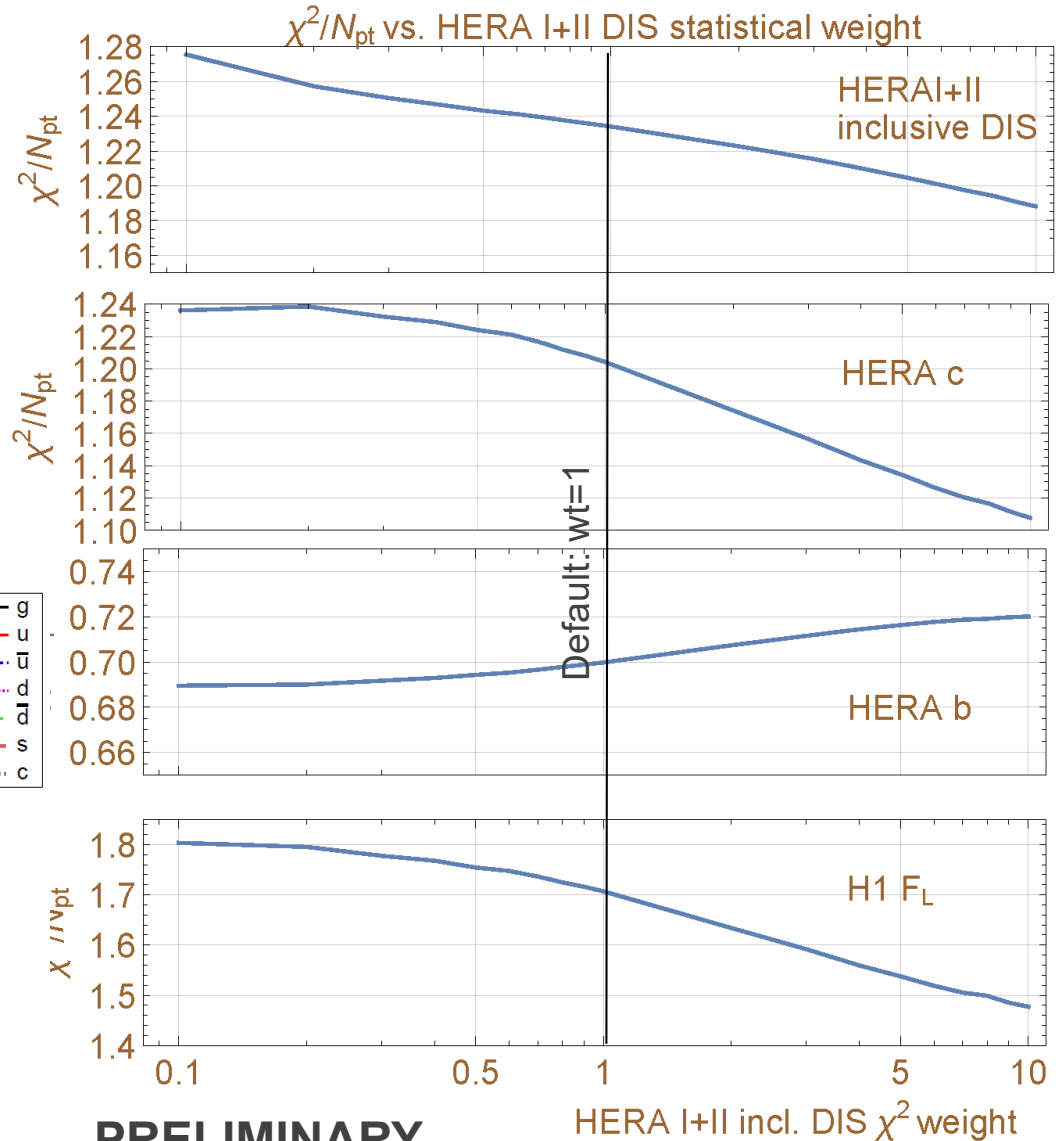
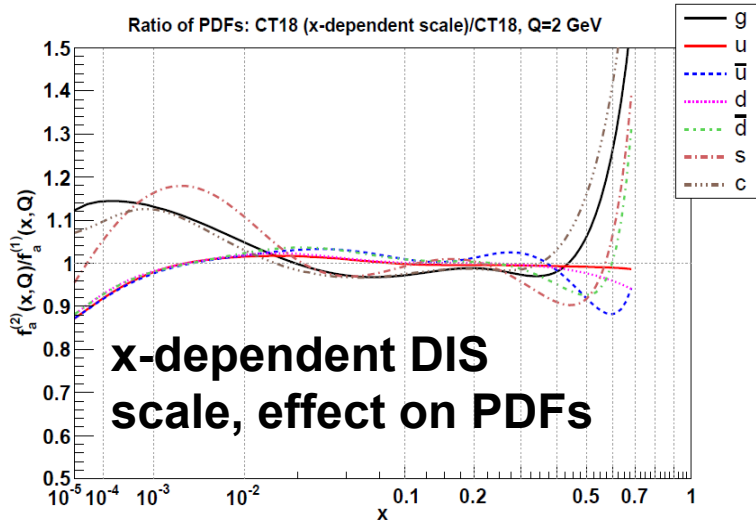
← The quadratic penalty for 162 systematic errors = 87.5

Fair (not perfect) agreement; can be mildly improved by the QCD scale choice

# CT18X and Z: a special factorization scale in DIS

The CT18Z fits uses a  $\mu_{DIS,X}$  scale that reproduces many features of NNLO-NLLx fits with  $\ln(1/x)$  resummation by the NNPDF [arXiv:1710.05935] and xFitter [1802.0064] groups.

$$\mu_{DIS,X}^2 = 0.8^2 \left( Q^2 + \frac{0.3 \text{ GeV}^2}{x^{0.3}} \right)$$

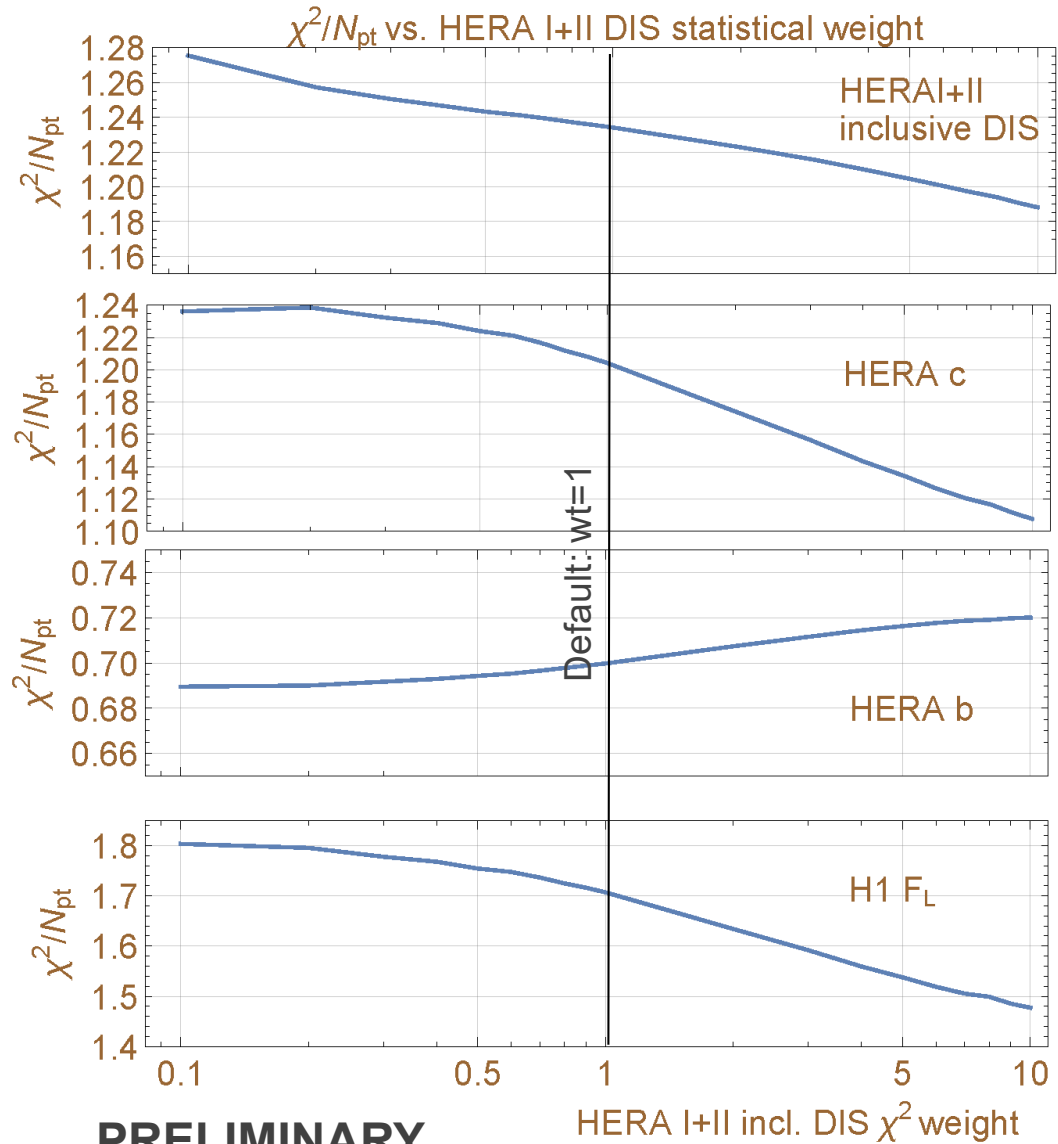


PRELIMINARY

# CT18X and Z: a special factorization scale in DIS

**Right:** when the  $\chi^2$  weight for the **inclusive** HERA I+II DIS is increased to  $wt = 10$  to suppress pulls from the other experiments,  $\chi_{CT18Z}^2/N_{pt}$  for HERA I+II DIS and HERA charm production decreases to about the same levels as in HERA-only NNLO+NLLx fits by other groups.

- **NNLO with an  $x$ -dependent scale is statistically indistinguishable from BFKL resummation in the CT18  $x$ -Q region ( $Q > 2$  GeV)**



# Theory input

Obs.	Expt.	fast table	NLO code	K-factors	R,F scales
Inclusive jet	ATL 7 CMS 7/8	APPLgrid fastNLO	NLOJet++	NNLOJet	$p_T, p_T^1$
$p_T^Z$	ATL 8	APPLgrid	MCFM	NNLOJet	$\sqrt{Q^2 + p_{T,Z}^2}$
W/Z rapidity W asymmetry	LHCb 7/8 ATL 7 CMS 8	APPLgrid	MCFM/aMCfast	FEWZ/MCFM	$M_{W,Z}$
DY (low,high mass)	ATL 7/8 CMS 8	APPLgrid	MCFM/aMCfast	FEWZ/MCFM	$Q_{ll}$
$t\bar{t}$	ATL 8 CMS 8	fastNNLO			$\frac{H_T}{4}, \frac{m_T}{2}$

when justified, a small Monte-Carlo error (typically 0.5%) added for NNLO/NLO K-factors

Theory calculations must be benchmarked before the PDF4LHC'20 combination!

One program/scale not sufficient for understanding theory uncertainties

2019-08-13

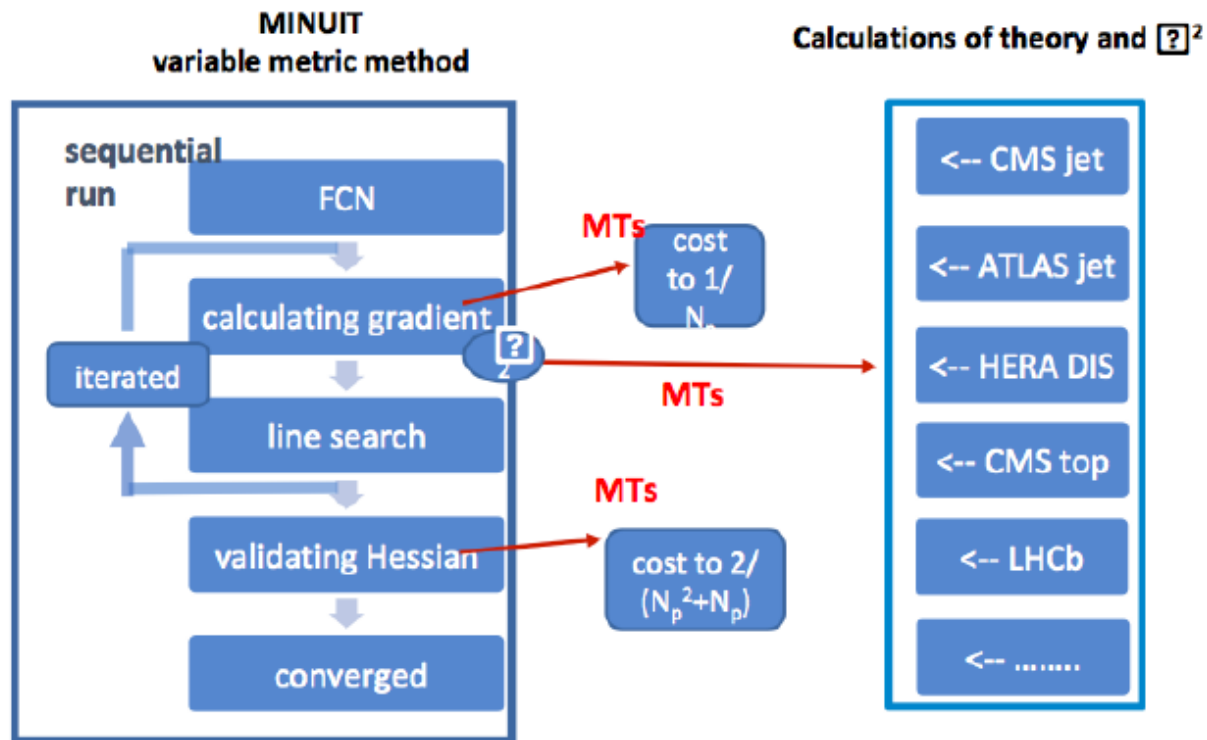
## Theoretical calculations for vector boson production

ID	Obs.	Expt.	fast table	NLO code	K-factors	$\mu_{R,F}$
245	$y_{\mu\mu}, \eta_\mu$	LHCb7ZW	APPLgrid	MCFM/aMCfast	MCFM/FEWZ	$M_{Z,W}$
246	$y_{ee}$	LHCb8Z				
250	$y_{\mu\mu}, \eta_\mu$	LHC8ZW				
249	$A(\mu)$	CMS8W				
253	$p_T^ll$	ATL8Z	APPLgrid	MCFM	NNLOJet	$M_T^ll$
201	$\sqrt{\tau}, y$	E605	CTEQ	FEWZ	$Q_{ll}$	$Q_{ll}$
203	$\sigma_{pd}/\sigma_{pp}, x_F$	E866				
204	$Q, x_F$	E866				
225	$A(e)$	CDF1Z	CTEQ	ResBos	$M_W$	$Q_{ll}$
227	$A(e)$	CDF2W				
234	$A(\mu)$	D02W				
281	$A(e)$	D02W				
260	$y_{ll}$	D02	CTEQ	VRAP	$Q_{ll}$	$Q_{ll}$
261	$y_{ll}$	CDF2				
266	$A(\mu)$	CMS7W	CTEQ	ResBos	$M_W$	$M_{Z,W}$
267	$A(e)$	CMS7W				
268	$y_{ll}, \eta_l, A(l)$	ATL7ZW(2012)				
248	$y_{ll}, \eta_l$	ATL7ZW(2016)				



# Fitting code parallelization with multi-threads

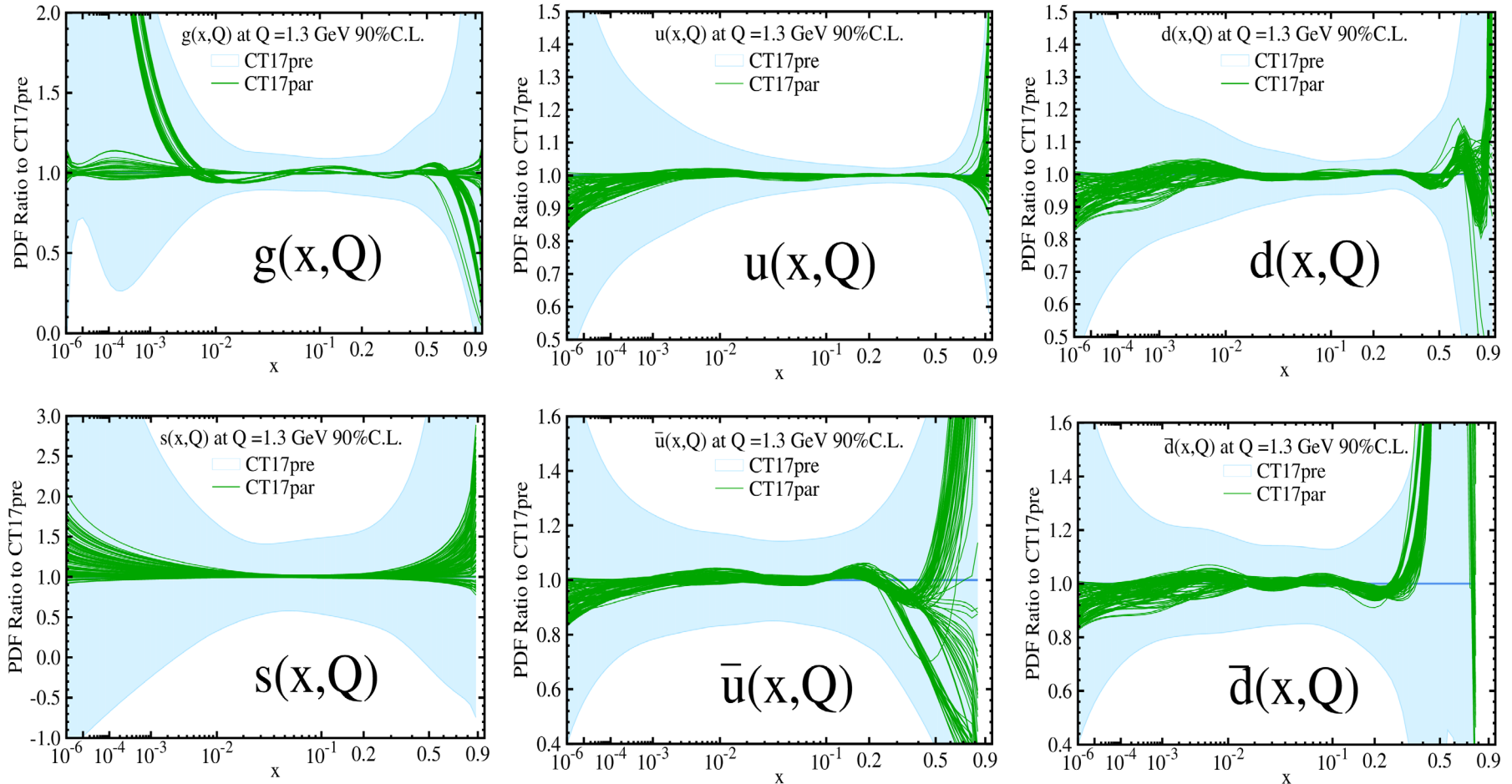
upgrade to a parallelized version of the fitting code, two-layer parallelization: 1. through rearrangement of the minimization algorithm; 2. via redistribution of the data sets



**Layer 1: after all a factor of 4~5 improvement on speed is achieved!**

**Layer 2: further speed up by a factor of 2, depending on data sets included**

# Explore various non-perturbative parametrization forms of PDFs



- CT17par – sample result of using various non-perturbative parametrization forms.
- No data constrain very large  $x$  or very small  $x$  regions.

# The questions we ask:

Which of 30+ eligible LHC experiments provide promising constraints on the CTEQ-TEA PDFs?

Do the LHC experiments agree among themselves and with other experiments?

# The questions we ask:

Which of 30+ eligible LHC experiments provide promising constraints on the CTEQ-TEA PDFs?

Do the LHC experiments agree among themselves and with other experiments?

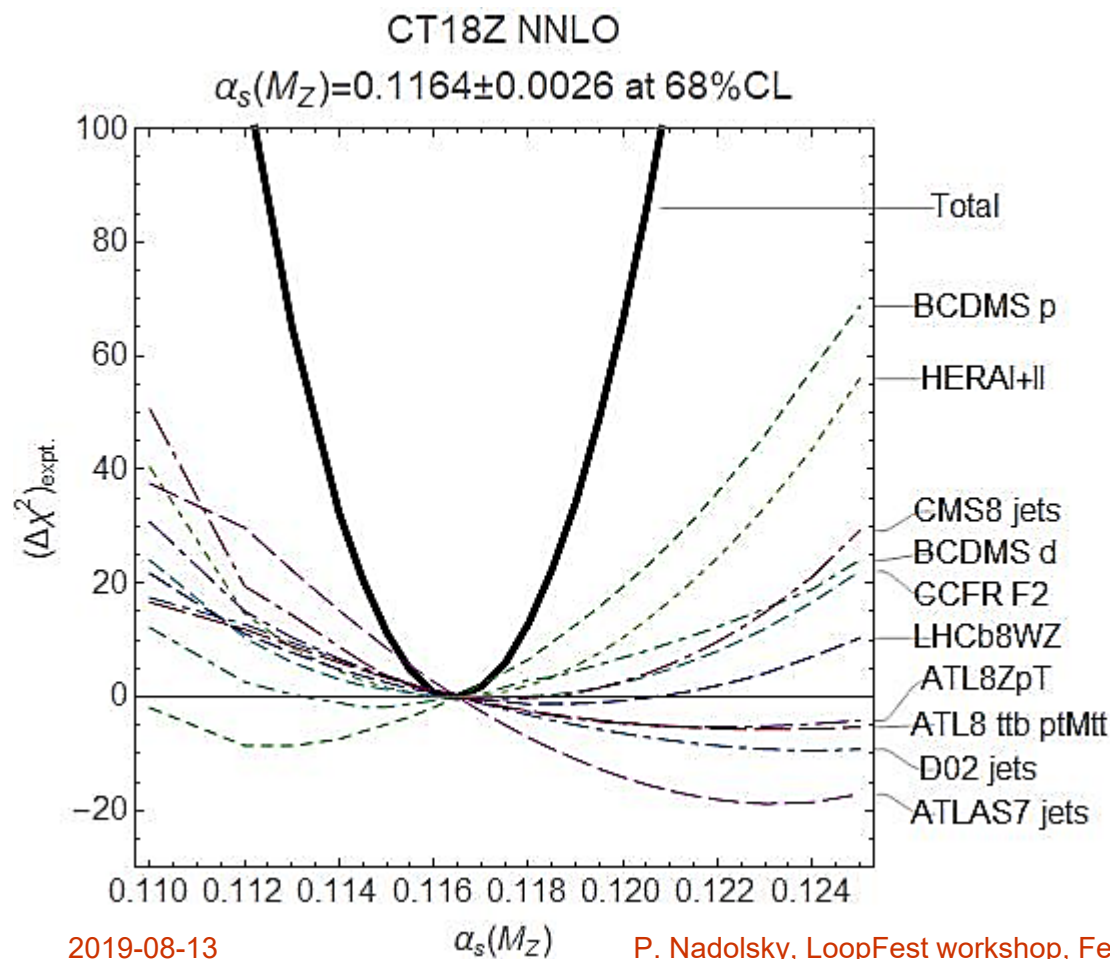
A **consistent** answer emerges from a powerful combination of four methods:

1. **Lagrange multiplier scans** } slow, most accurate
  2. **PDFSense and  $L_2$  sensitivity** }
  3. **ePump** [Schmidt, Pumplin, Yuan, PRD 98, 094005] }
  4. **Effective Gaussian variables** }
- Fast approximations

# Lagrange Multiplier (LM) Scan: $\alpha_s(M_Z)$

The LM scan technique is introduced in **Stump et al., Phys.Rev. D65 (2001) 014012**

😊 Detailed dependence of  $\chi^2$       😞 slow; refitting on a supercomputing cluster



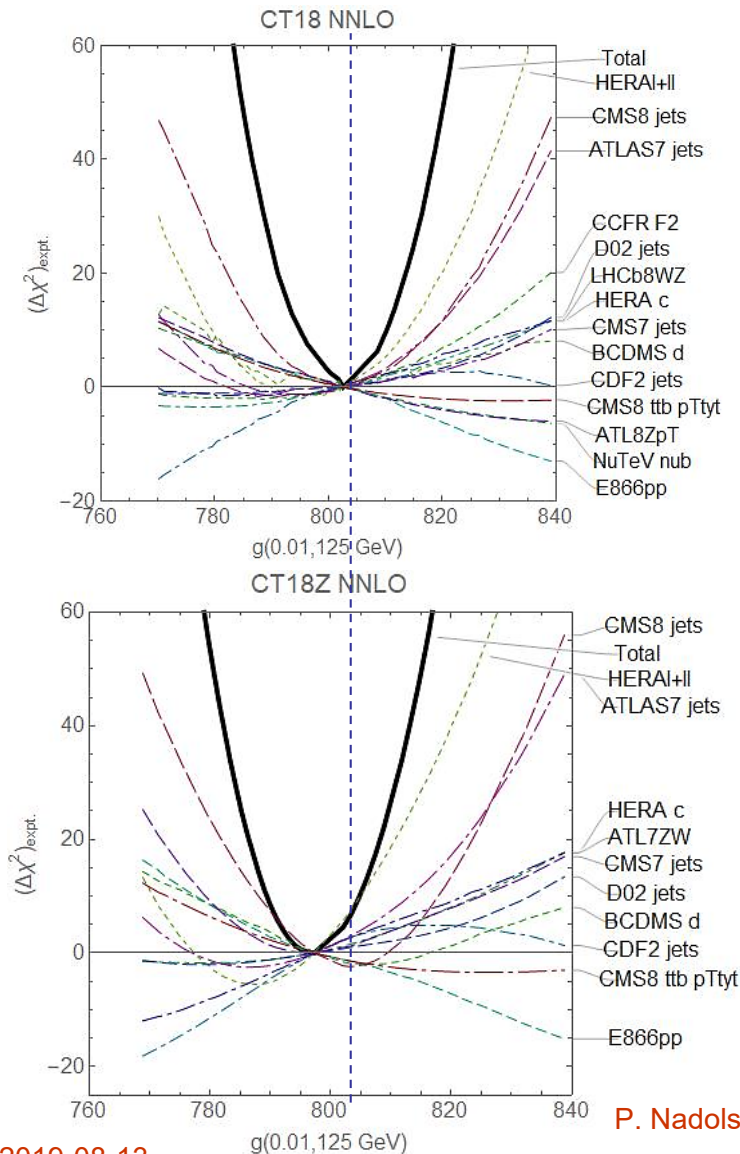
Examine changes in  $\chi^2$  for

- all experiments (“Total”)
- individual experiments

$\alpha_s(m_Z)$  from global fit closer to 0.117 than to 0.118, primarily due to pulls from HERA and BCDMS DIS experiments



# Lagrange Multiplier scan: $g(0.01, 125 \text{ GeV})$



## Upper row: CT18

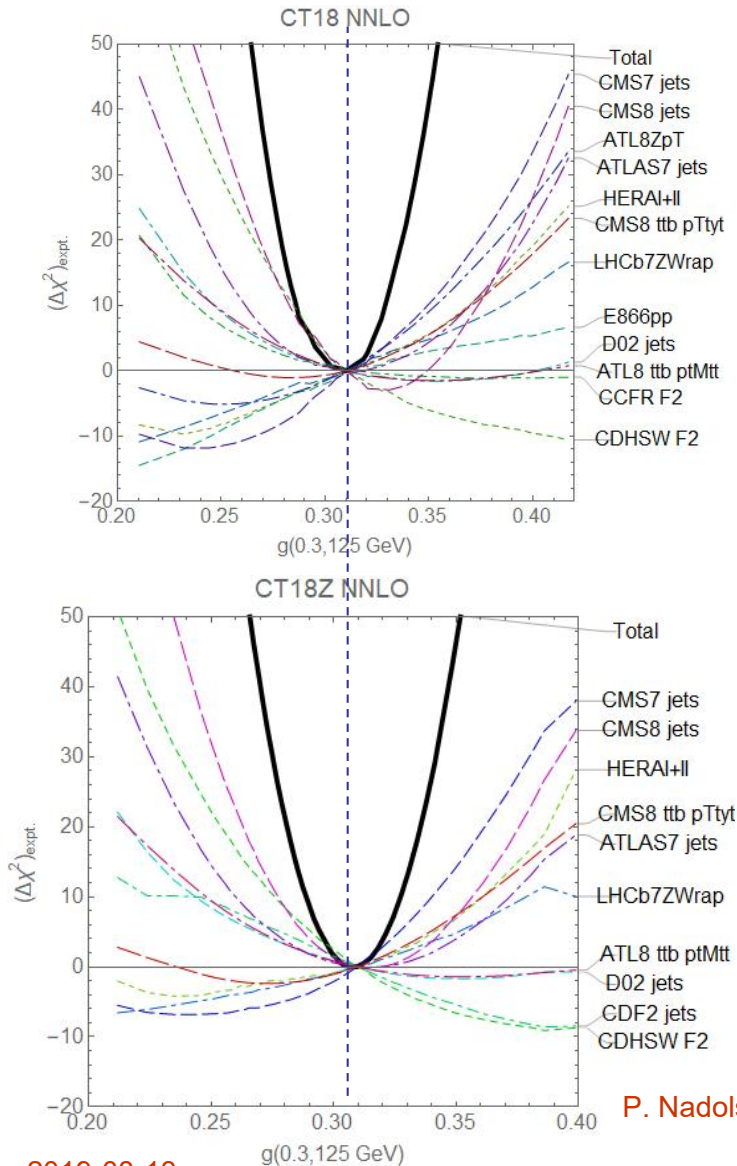
6500 core hours

- HERAI+II data set provides the dominant constraint, followed by ATLAS, CDF2, CMS, D02 jet production, HERA charm,...
- $t\bar{t}$  double-diff. cross sections provide weaker constraints

## Lower row: CT18Z

- CT18Z: a 1% lower NNLO gluon in the Higgs production region than for CT14/CT18

# Lagrange Multiplier scan: $g(0.3, 125 \text{ GeV})$



Upper/lower rows: CT18/CT18Z

Good overall agreement. But observe opposite pulls from ATLAS7/CMS7 jet production and CMS8 jet production

Similarly, ATLAS  $t\bar{t}$  distributions  $d^2\sigma/(dp_{T,t}dm_{t\bar{t}})$  and CMS  $t\bar{t}$  distributions  $d^2\sigma/(dp_{T,t}dy_{t,ave})$  at 8 TeV impose weak opposite pulls

Constraints from ATLAS 8  $Z p_T$  production data are moderate and still affected by NNLO scale uncertainty

# PDFSense **program**

Approximate LM scans, **fast... and many other insights**

# PDFSense program: fast surveys of QCD data using a vector data technique

**Authors:** Tim Hobbs, Bo Ting Wang, et al.: arXiv:1803.02777,  
1904.00222, 1907.00988

**Language:** Mathematica

**Inputs:** vectors of fitted data residuals  $r_i(\vec{a}) \equiv [T_i(\vec{a}) - D_i^{shifted}(\vec{a})]/\sigma_i$   
and predicted cross sections evaluated for Hessian or MC error PDFs

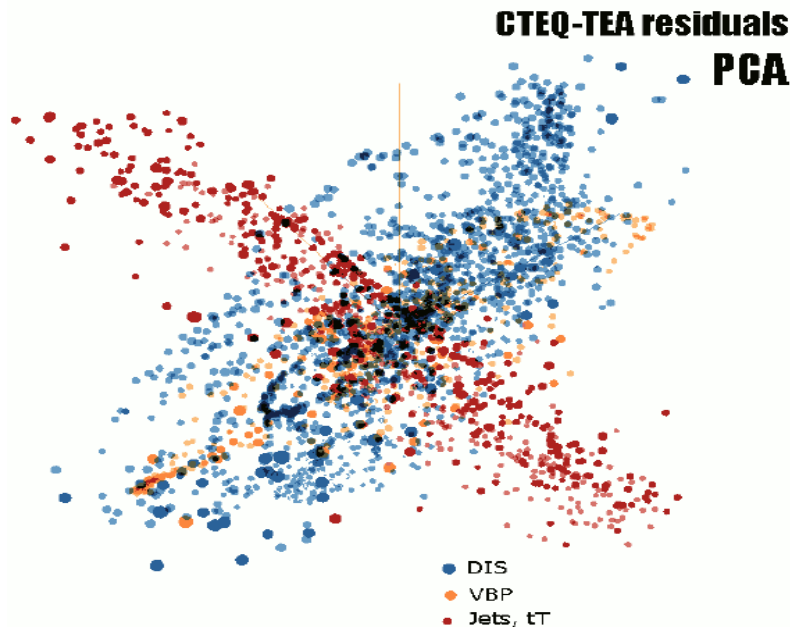
**Outputs:** Hessian **sensitivity** variables  $S_f$  and  $S_{f,L2}$ : easy-to-compute  
indicators of data point sensitivity to PDFs in the presence of  
experimental errors

**Available by request**

Definitions in the backup

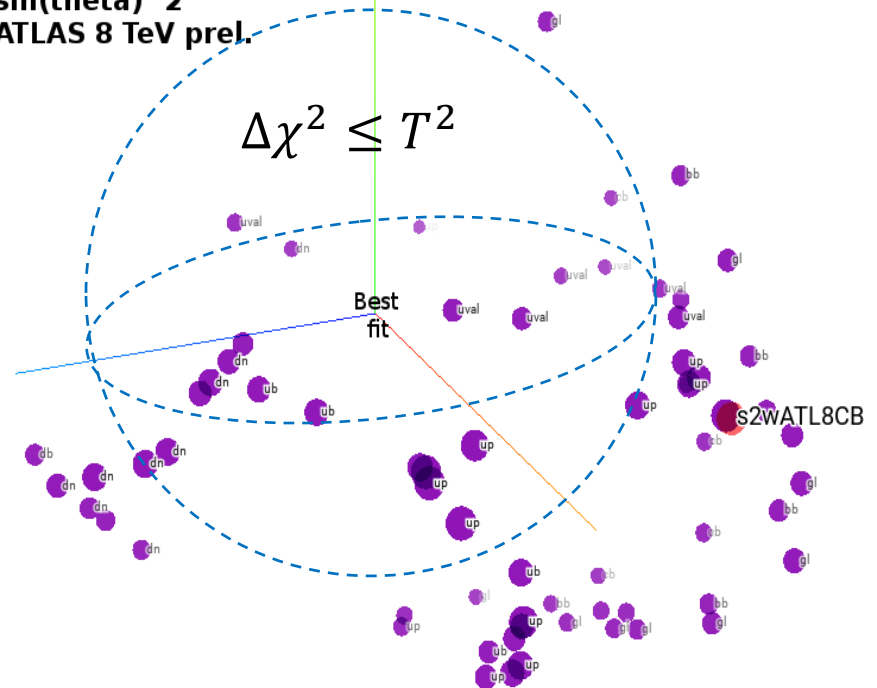
# Vectors of data point residuals...

... carry detailed information about sensitivity of individual experimental data points to PDFs; can be studied using statistical packages (TensorFlow, Mathematica,...)



Principal Component Analysis (PCA) visualizes the 56-dim. manifold by reducing it to 10 dimensions (à la META PDFs)

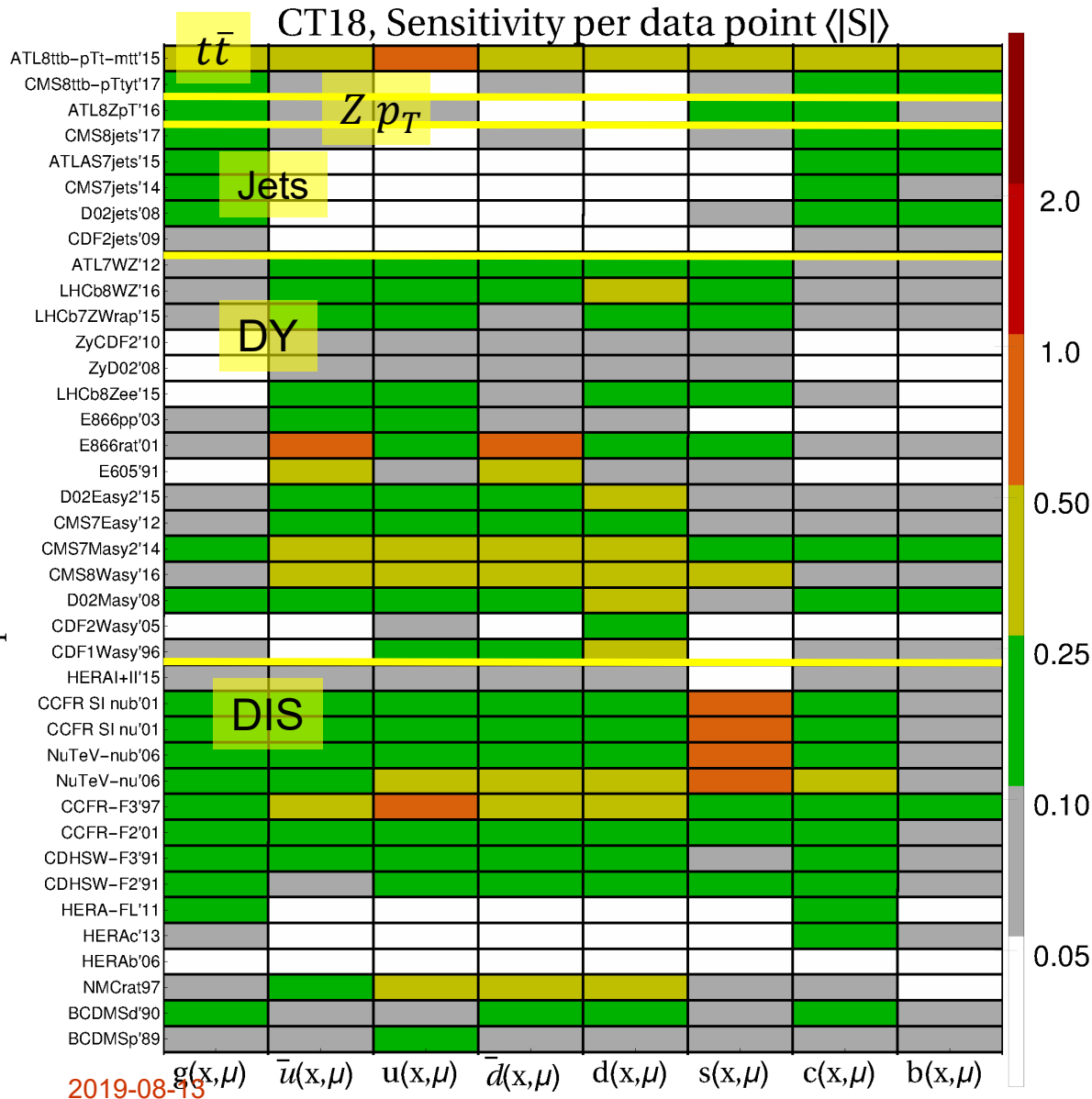
CT14 NNLO PDF variations with the largest correlation with  $\sin(\theta)^2$  ATLAS 8 TeV prel.



Using Hessian PDFs



# Sensitivity of hadronic experiments to PDFs



Computed using the  
**PDFSense** method  
[arXiv:0803.02777]

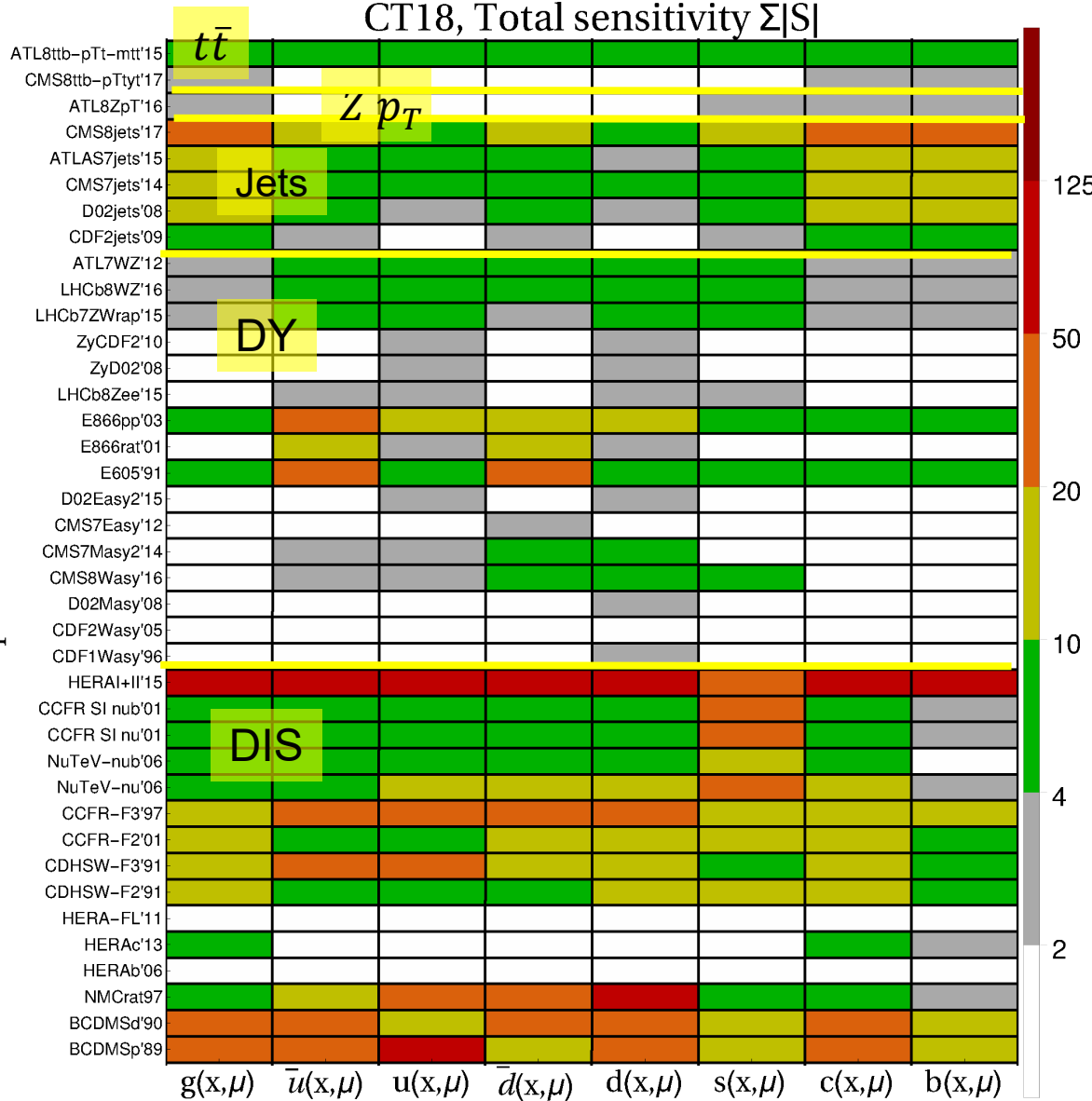
Average sensitivity to  
 $f_a(x_i, \mu_i)$  **per data  
point**

- defined in the backup
- expt. and PDF errors included

**Red bars =  
most sensitive  
experiments**

# Sensitivity of hadronic experiments to PDFs

CT18, Total sensitivity  $\Sigma|S|$

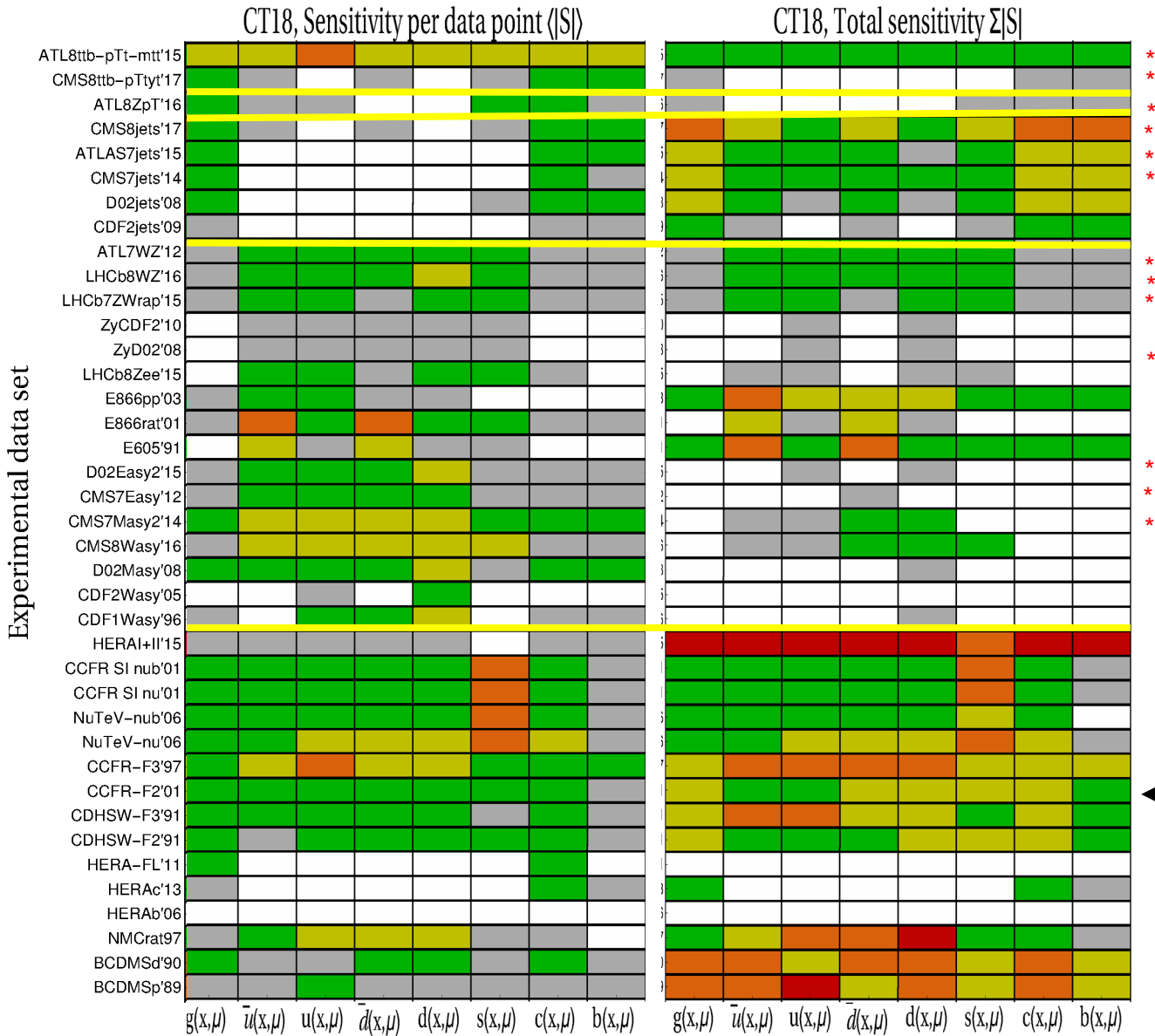


Total sensitivity to  $f_a(x_i, \mu_i)$ , summed over data points

$$\sum_{\text{points}} |S_{f,i}|$$

Computed using the PDFSense code [arXiv:0803.02777]

# Sensitivity of hadronic experiments to PDFs



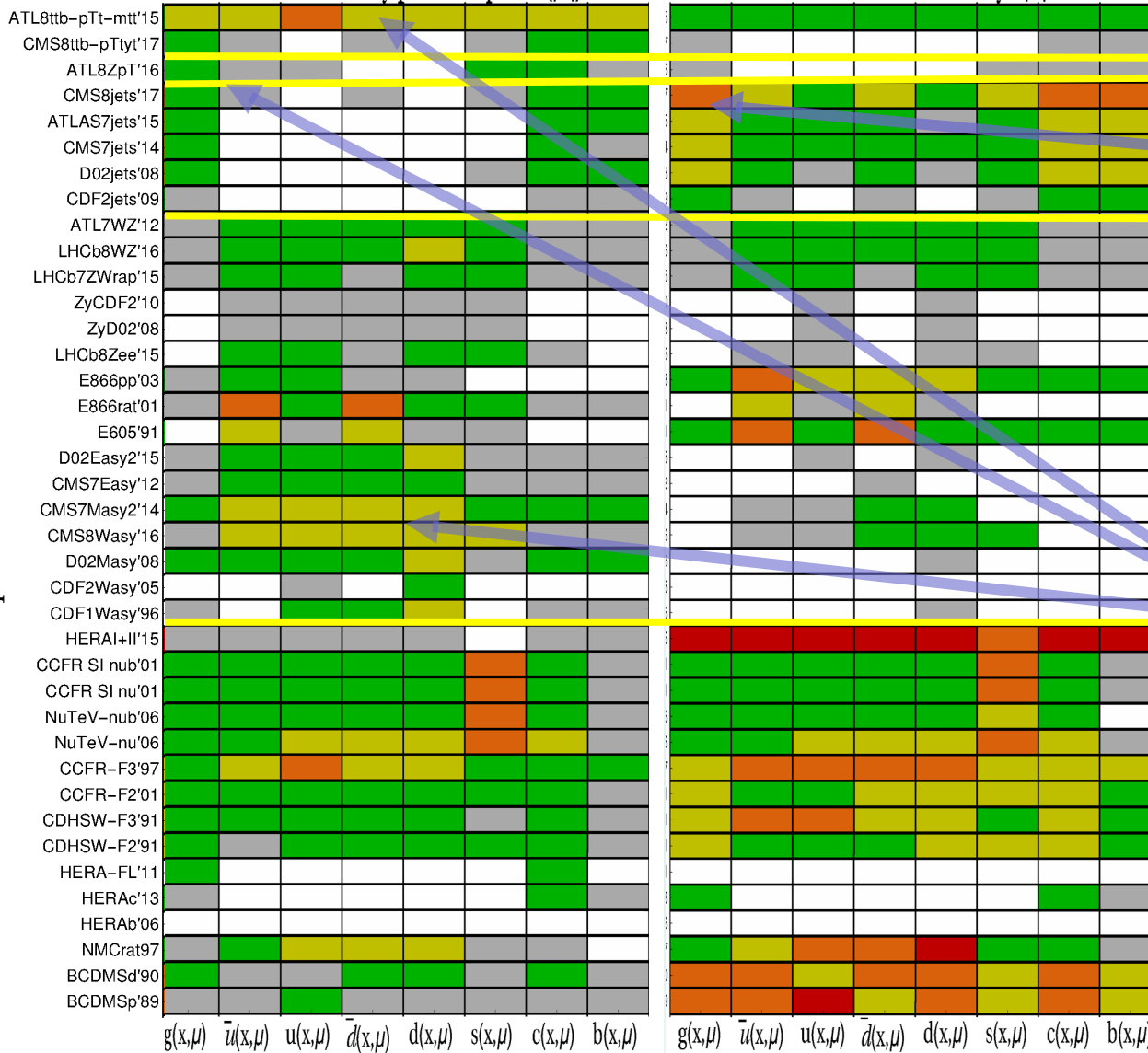
The LHC data sets (\*) hold a great promise – if they agree

HERA I+II, BCDMS, NMC, DIS data sets dominate experimental constraints. Large numbers of data points matter!

# Sensitivity of hadronic experiments to PDFs

CT18, Sensitivity per data point  $\langle |S| \rangle$

CT18, Total sensitivity  $\sum |S|$



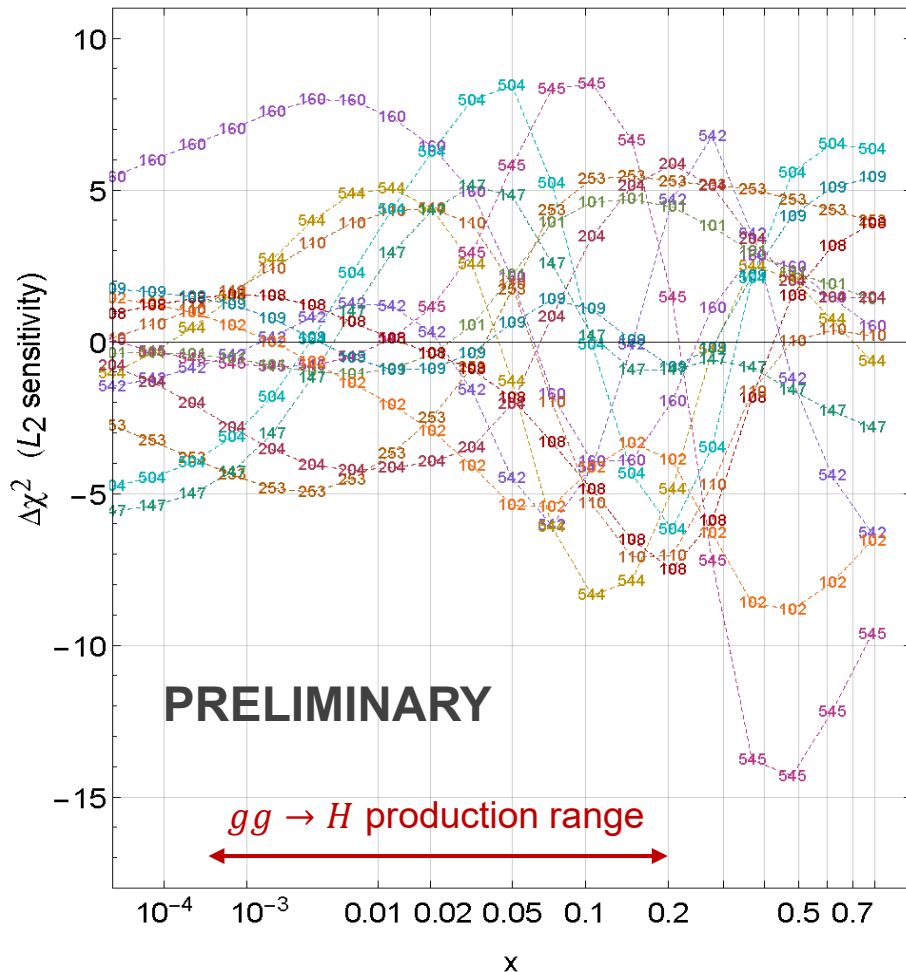
CMS 7 & 8 TeV single-inclusive jet production has highest total sensitivity ( $N_{pt} > 100$ ), modest sensitivity per data point

$t\bar{t}$ , CMS  $W$  asy, high- $p_T$   $Z$  production have high sensitivity per data point, smaller total sensitivity ( $N_{pt} \sim 10 - 20$ )

# Estimated $\chi^2$ pulls from experiments

( $L_2$  sensitivity, arXiv:1904.00222, v. 2)

CT18 NNLO,  $g(x, 100 \text{ GeV})$



CT18 NNLO, gluon at  $Q=100 \text{ GeV}$

**15 core-minutes**

Most sensitive experiments

- 253--- ATL8ZpTbT
- 542--- CMS7jtR7y6T
- 544--- ATL7jtR6uT
- 545--- CMS8jtR7T
- 160--- HERAIpII
- 101--- BcdF2pCor
- 102--- BcdF2dCor
- 108--- cdhswf2
- 109--- cdhswf3
- 110--- ccfif2.mi
- 147--- Hn1X0c
- 204--- e866ppxf
- 504--- cdf2jtCor2

Experiments with large  $\Delta\chi^2 > 0$  [ $\Delta\chi^2 < 0$ ] pull  $g(x, Q)$  in the negative [positive] direction at the shown  $x$

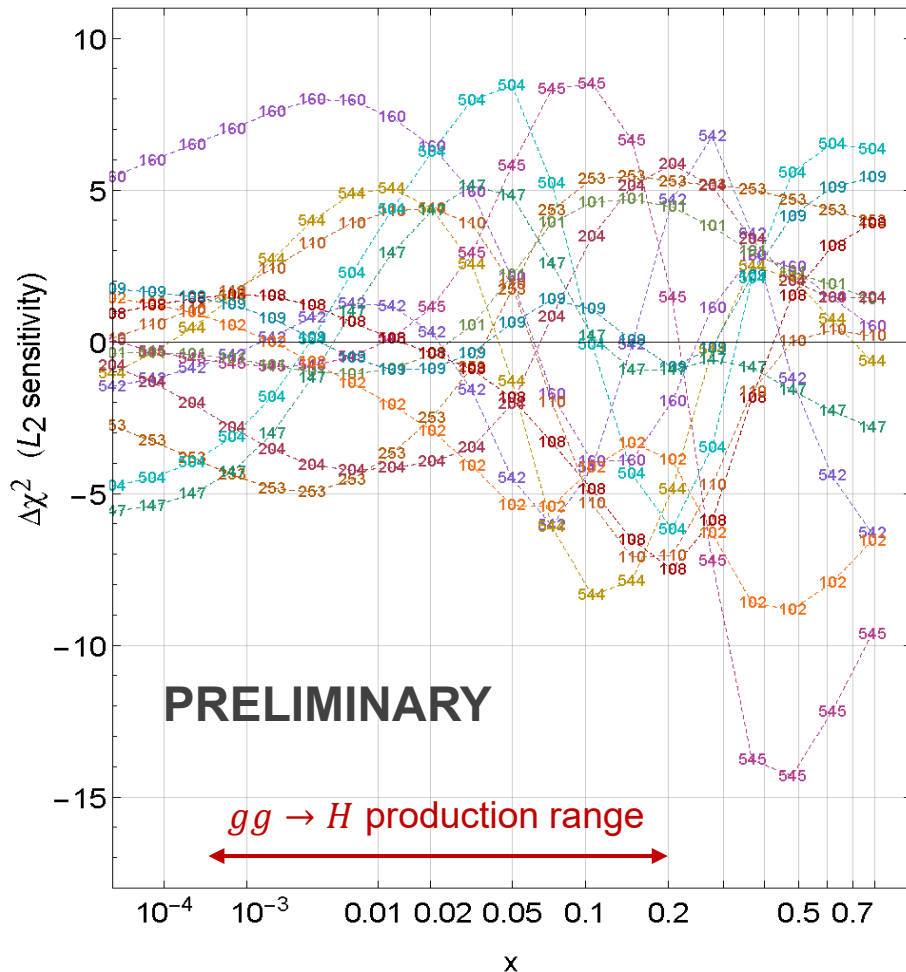
Estimated using CT18 Hessian PDFs



# Estimated $\chi^2$ pulls from experiments

( $L_2$  sensitivity, arXiv:1904.00222, v. 2)

CT18 NNLO,  $g(x, 100 \text{ GeV})$



CT18 NNLO, gluon at  $Q=100 \text{ GeV}$

Most sensitive experiments

- 253--- ATL8ZpTbT
- 542--- CMS7jtR7y6T
- 544--- ATL7jtR6uT
- 545--- CMS8jtR7T
- 160--- HERAIpII
- 101--- BcdF2pCor
- 102--- BcdF2dCor
- 108--- cdhswf2
- 109--- cdhswf3
- 110--- ccfir2.mi
- 147--- Hn1X0c
- 204--- e866ppxf
- 504--- cdf2jtCor2

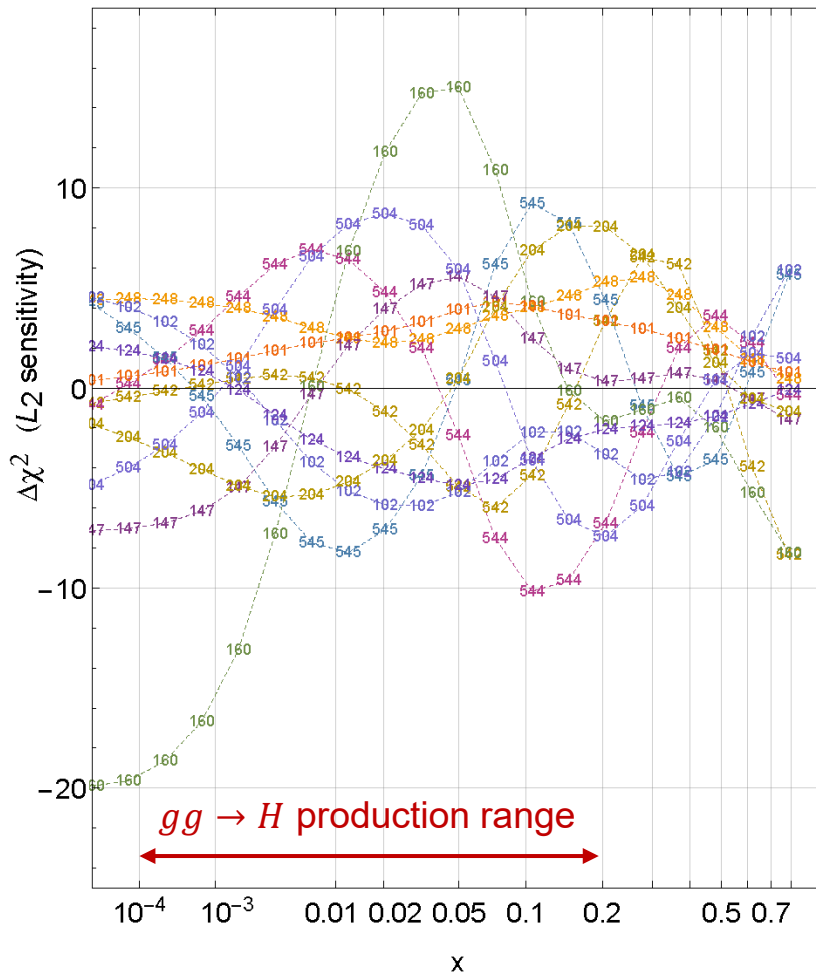
Note opposite pulls (tensions) in some  $x$  ranges between HERA I+II DIS (ID=160); CDF (504), ATLAS 7 (544), CMS 7 (542), CMS 8 jet (545) production; E866pp DY (204); ATLAS 8 Z pT (253) production; BCDMS and CDHSW DIS

# Estimated $\chi^2$ pulls from experiments

( $L_2$  sensitivity, arXiv:1904.00222, v. 2)

CT18Z NNLO,  $g(x, 100 \text{ GeV})$

Same for CT18Z NNLO



Most sensitive experiments

- 248--- ATL7ZW.xF
- 542--- CMS7jtR7y6T
- 544--- ATL7jtR6uT
- 545--- CMS8jtR7T
- 160--- HERA I+II DIS
- 101--- BcdF2pCor
- 102--- BcdF2dCor
- 124--- NuTvNuChXN
- 147--- Hn1X0c
- 204--- e866ppxf
- 504--- cdf2jtCor2

Constraints from HERA I+II DIS (ID=160) follow a different trend from CT18 NNLO because of the  $x$  –dependent QCD scale

**PRELIMINARY**

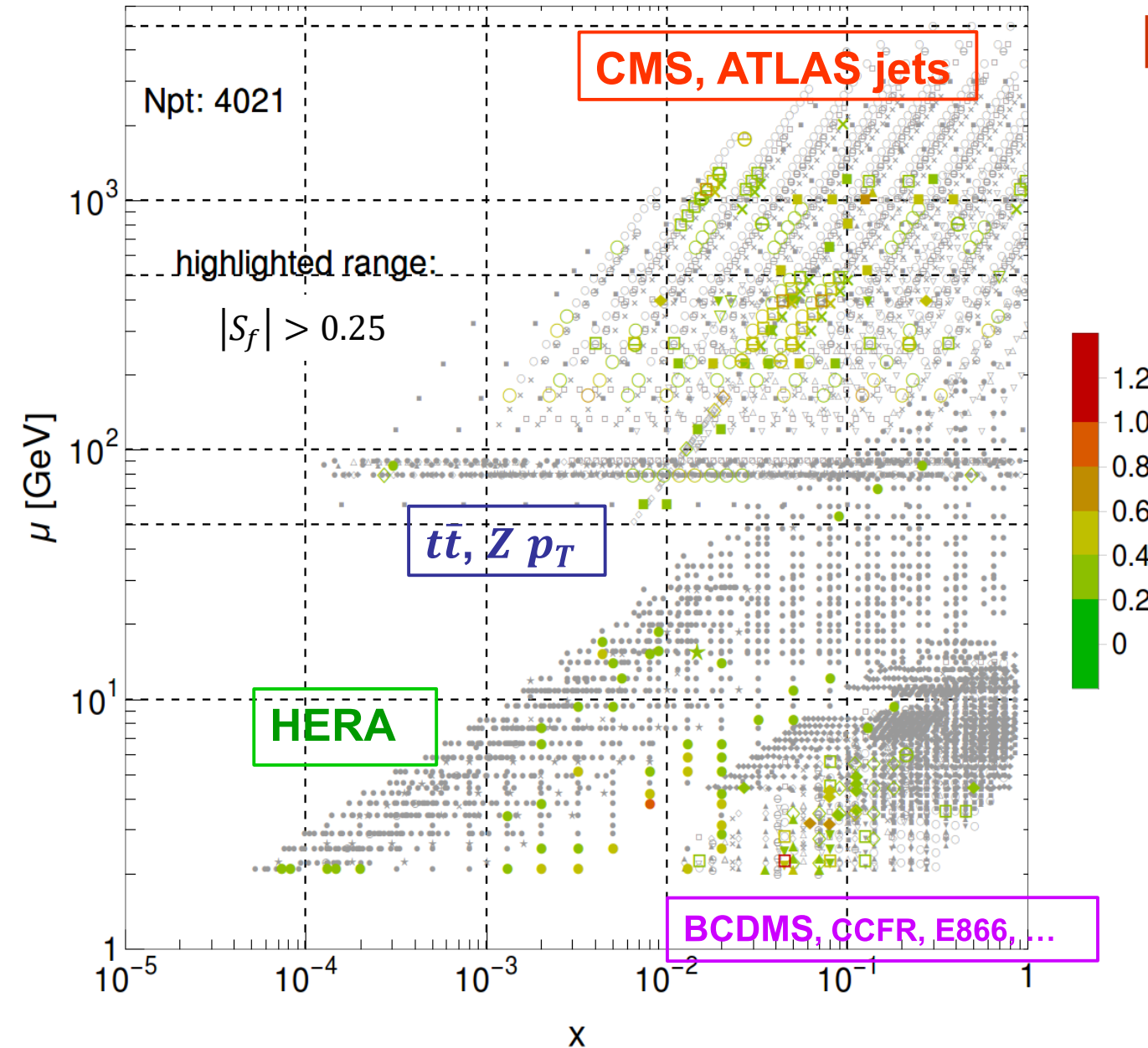
$|S_f|$  for  $\sigma(H^0)$ , 14 TeV, CT14HERA2NNLO

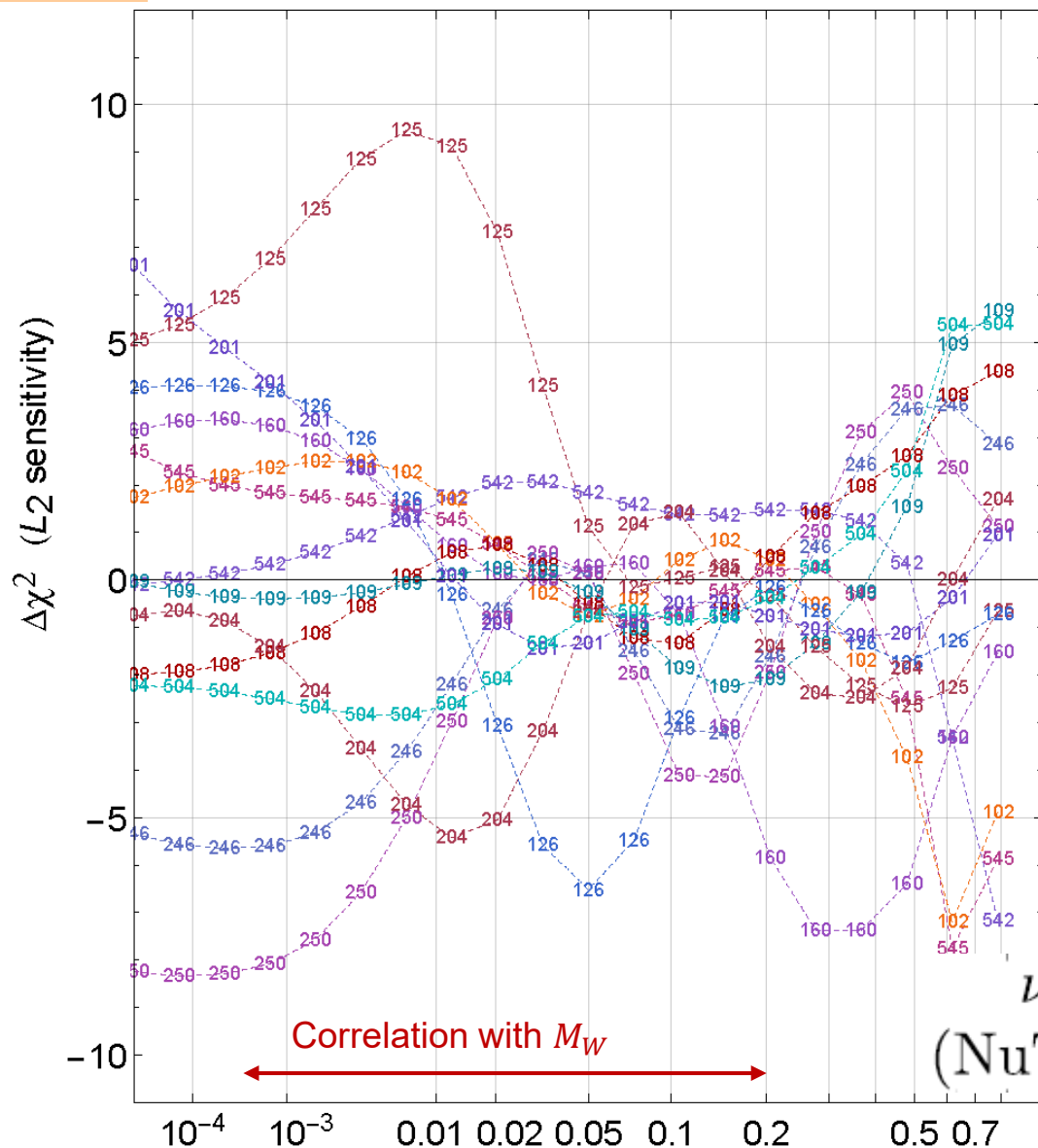
# Higgs boson production

HERA DIS still has the **dominant sensitivity!**

CMS 8 TeV jets is the next expt. after HERA sensitive to  $\sigma_H(14 \text{ TeV})$ ; jet scale uncertainty dampens  $|S_f|$  for jets

Good correlations  $C_f$  with some points in E866, BCDMS, CCFR, CMS WASY,  $Z p_T$  and  $t\bar{t}$  production; but not as many points with high  $|S_f|$  in these processes





2019-08-13

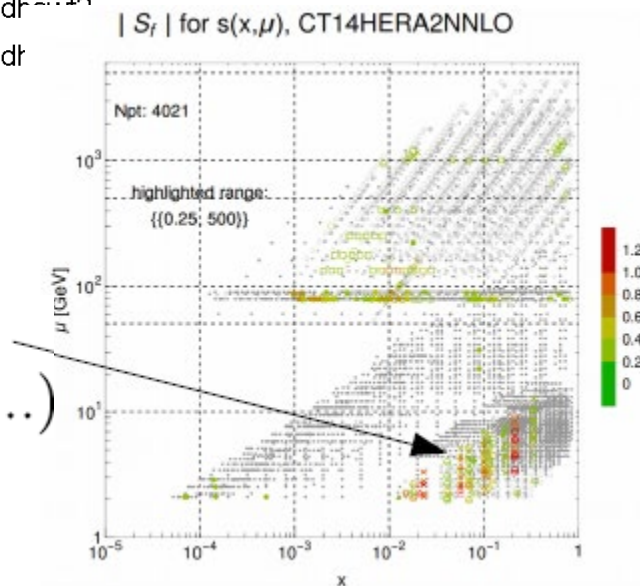
X P. Nadolsky, LoopFest workshop, Fermilab

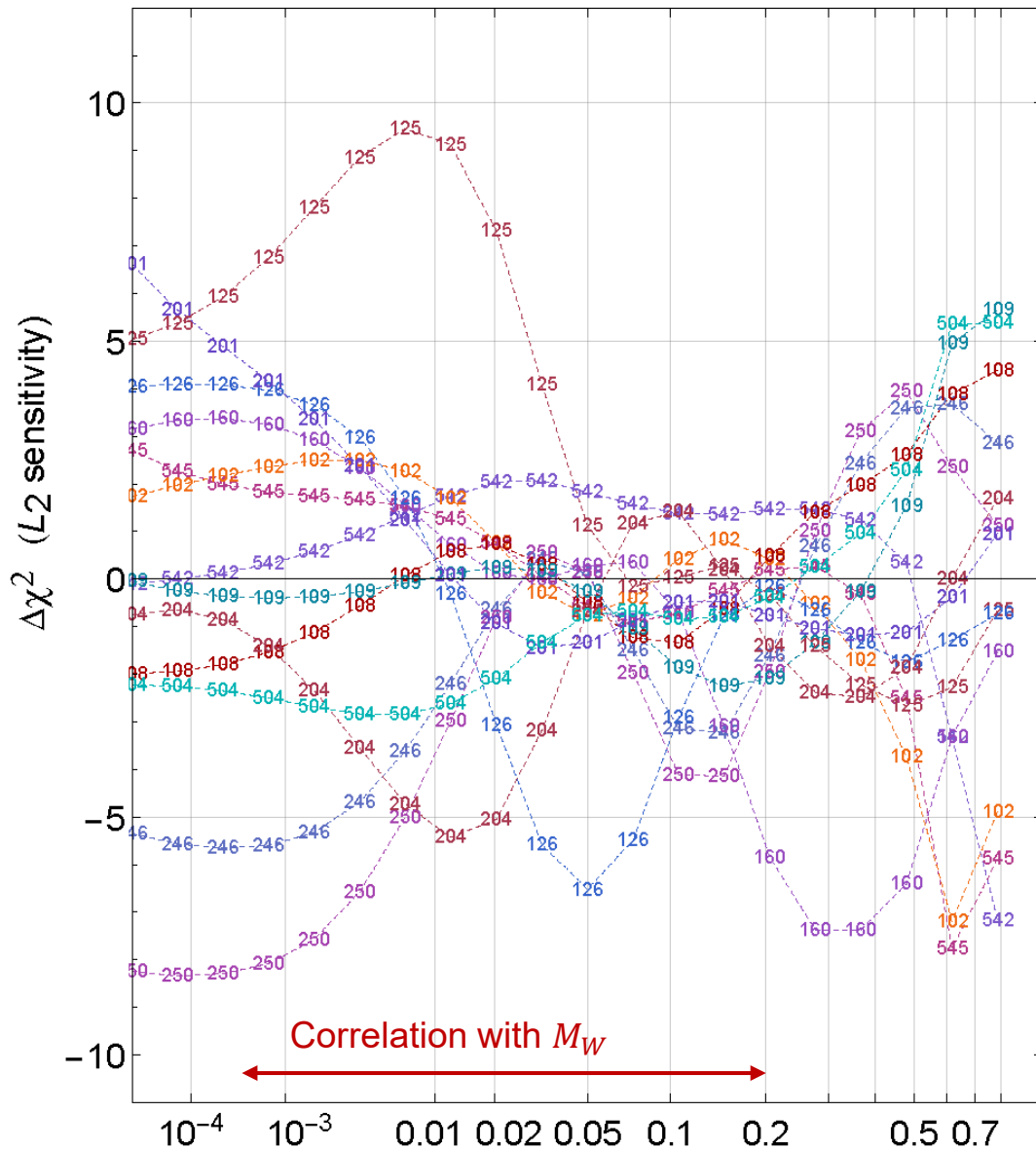
This analysis can be extended to strangeness, which affects  $M_W$  extraction through  $Z$  boson recoil calibration

### Most sensitive experiments

- 246--- LHCb8Zeer
- 250--- LHCb8WZ
- 542--- CMS7jtR7y6T
- 545--- CMS8jtR7T
- 160--- HERAplI
- 102--- BcdF2dCor
- 108--- cdh
- 109--- cdh
- 125--- NuTvNbChXN
- 126--- CcfrNuChXN
- 201--- e605
- 204--- e866ppxf
- 504--- cdf2jtCor2

$\nu$ DIS  
(NuTeV, ...)



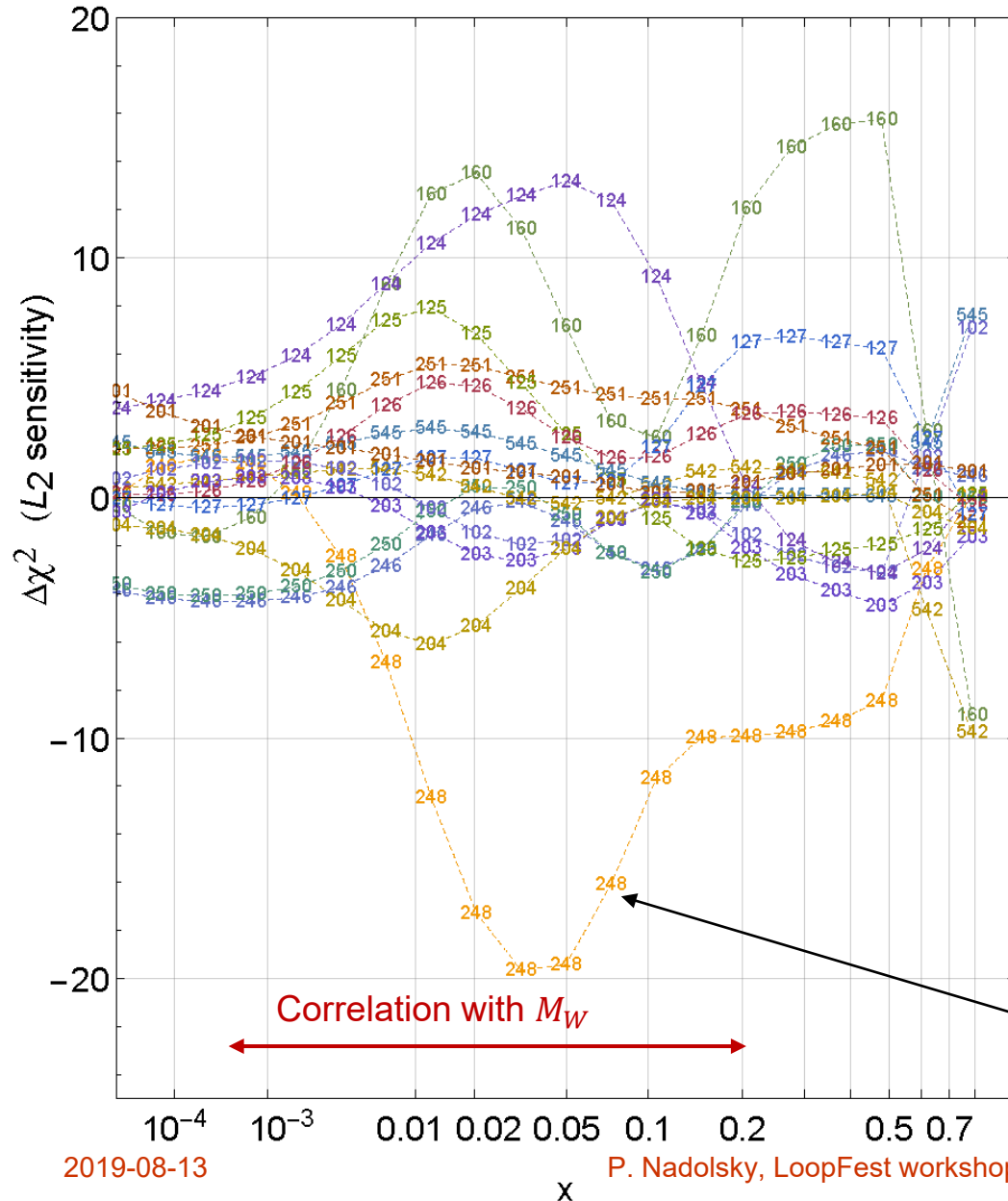


This analysis can be extended to strangeness, which affects  $M_W$  extraction through  $Z$  boson recoil calibration

### Most sensitive experiments

- 246--- LHCb8Zeer
- 250--- LHCb8WZ
- 542--- CMS7jtR7y6T
- 545--- CMS8jtR7T
- 160--- HERAplI
- 102--- BcdF2dCor
- 108--- cdhswf2
- 109--- cdhswf3
- 125--- NuTeVNbChXN
- 126--- CcfrNuChXN
- 201--- e605
- 204--- e866ppxf
- 504--- cdf2jtCor2

A tension trend between DIS (NuTeV, CCFR, HERA) and Drell-Yan (LHCb W/Z, E866 pp, ...) experiments



## Most sensitive experiments

- 246--- LHCb8Zeer
- 248--- ATLAS7Z/W
- 250--- LHCb8WZ
- 251--- ATLAS8DY
- 542--- CMS7jtR7y6T
- 545--- CMS8jtR7T
- 160--- HERA I+II
- 102--- BcdF2dCor
- 124--- NuTeVChXN
- 125--- NuTeVNbChXN
- 126--- CcfrNuChXN
- 127--- CcfrNbChXN
- 201--- e605
- 203--- e866f
- 204--- e866ppxf

A tension trend between DIS (HERA I+II, CCFR, NuTeV) and Drell-Yan (ATLAS 7 Z/W, LHCb W/Z, E866 pp, ...) experiments

pronounced pull of ATLAS7 Z/W data



# Key points, the CT18(Z) global QCD analysis

- modest reduction in the PDF uncertainties compared to CT14
- DIS experiments dominate constraints on PDFs
- LHC Run-1 and 2 processes (jet,  $W/Z$ , high- $p_T$   $Z$ ,  $t\bar{t}$ ,  $W + c$ , ...production) will provide promising constraints once they are brought into mutual agreement
- NNLO DIS cross sections with an  $x$ -dependent factorization scale behave like NNLO+NNLx resummed ones, are incorporated in CT18Z PDFs with the modified small- $x$  gluon and strangeness
- **Future reduction of NNLO PDF uncertainties is not automatic. The goals of the HL-LHC program demand a broad coordinated effort to eliminate tensions between experimental measurements that were identified using several techniques ( $L_2$  sensitivity, LM scans,...)**



# Backup

# CT18(Z), $\chi^2$ values

ID#	Experimental data set	$N_{pt,n}$	$\chi_n^2$	$\chi_n^2/N_{pt,n}$	$S_n$
160	HERAI+II 1 fb <sup>-1</sup> , H1 and ZEUS NC and CC e <sup>±</sup> p reduced cross sec. comb. [32]	1120	1405.1(1370.2)	1.25(1.22)	5.6(5.0)
101	BCDMS F <sub>2</sub> <sup>P</sup> [33]	337	376.3(385.8)	1.12(1.14)	1.5(1.8)
102	BCDMS F <sub>2</sub> <sup>D</sup> [34]	250	288.3(289.3)	1.15(1.16)	1.7(1.7)
104	NMC F <sub>2</sub> <sup>d</sup> /F <sub>2</sub> <sup>p</sup> [35]	123	123.3(114.5)	1.00(0.93)	0.061(-0.51)
108	CDHSW <sup>†</sup> F <sub>2</sub> <sup>P</sup> [36]	85	85.1	1.00	0.061
109	CDHSW <sup>†</sup> F <sub>2</sub> <sup>D</sup> [36]	96	83.1	0.865	-0.93
110	CCFR F <sub>2</sub> <sup>P</sup> [37]	69	78.3(74.6)	1.13(1.08)	0.81( 0.52)
111	CCFR xF <sub>3</sub> <sup>P</sup> [38]	86	33.7(29.5)	0.391(0.343)	-5.3(-5.9)
124	NuTeV νμμ SIDIS [39]	38	19.3(29.7)	0.508(0.781)	-2.6(-0.96)
125	NuTeV ν̄μμ SIDIS [39]	33	36.5(54.7)	1.11(1.66)	0.50( 2.3)
126	CCFR νμμ SIDIS [40]	40	29.2(33.0)	0.729(0.825)	-1.3(-0.76)
127	CCFR ν̄μμ SIDIS [40]	38	20.1(20.8)	0.530(0.550)	-2.4(-2.3)
145	H1 σ <sub>p</sub> <sup>2</sup> [41]	10	6.8(7.1)	0.682(0.710)	-0.65(-0.57)
147	Combined HERA charm production [42]	47	58.6(54.7)	1.25(1.16)	1.2( 0.82)
169	H1 F <sub>L</sub> [43]	9	17.1(14.5)	1.90(1.61)	1.7( 1.2)
201	E605 Drell-Yan process [44]	119	100.3(98.0)	0.843(0.824)	-1.2(-1.4)
203	E866 Drell-Yan process σ <sub>pd</sub> /(2σ <sub>pp</sub> ) [45]	15	10.0(12.2)	0.670(0.813)	-0.90(-0.43)
204	E866 Drell-Yan process Q <sup>2</sup> d <sup>2</sup> σ <sub>pp</sub> /(dQdxF) [46]	184	240.2(239.3)	1.31(1.30)	2.7( 2.7)
225	CDF Run-1 electron A <sub>ch</sub> , p <sub>Tℓ</sub> > 25 GeV [47]	11	9.1(9.2)	0.828(0.835)	-0.28(-0.27)
227	CDF Run-2 electron A <sub>ch</sub> , p <sub>Tℓ</sub> > 25 GeV [48]	11	13.6(13.3)	1.23(1.21)	0.65( 0.61)
234	DØ Run-2 muon A <sub>ch</sub> , p <sub>Tℓ</sub> > 20 GeV [49]	9	9.3(9.2)	1.04(1.02)	0.23( 0.19)
260	DØ Run-2 Z rapidity [50]	28	17.0(19.0)	0.606(0.680)	-1.6(-1.3)
261	CDF Run-2 Z rapidity [51]	29	49.6(62.6)	1.71(2.16)	2.3( 3.4)
266	CMS 7 TeV 4.7 fb <sup>-1</sup> , muon A <sub>ch</sub> , p <sub>Tℓ</sub> > 35 GeV [52]	11	8.6(13.5)	0.785(1.23)	-0.40( 0.64)
267	CMS 7 TeV 840 pb <sup>-1</sup> , electron A <sub>ch</sub> , p <sub>Tℓ</sub> > 35 GeV [53]	11	12.2(16.8)	1.11(1.53)	0.39( 1.2)
268	ATLAS 7 TeV 35 pb <sup>-1</sup> W/Z cross sec., A <sub>ch</sub> [54]	41	44.1	1.08	0.41
281	DØ Run-2 9.7 fb <sup>-1</sup> electron A <sub>ch</sub> , p <sub>Tℓ</sub> > 25 GeV [55]	13	24.4(20.8)	1.88(1.60)	1.9(1.4)
504	CDF Run-2 inclusive jet production [56]	72	109.9(107.6)	1.53(1.49)	2.8(2.6)
514	DØ Run-2 inclusive jet production [57]	110	114.4(115.9)	1.04(1.05)	0.33(0.43)

245	LHCb 7 TeV 1.0 fb <sup>-1</sup> W/Z forward rapidity cross sec. [23]	33	50.8(41.4)	1.54(1.25)	2.0(1.0)
246	LHCb 8 TeV 2.0 fb <sup>-1</sup> Z → e <sup>-</sup> e <sup>+</sup> forward rapidity cross. sec. [24]	17	23.4(21.1)	1.37(1.24)	1.1(0.8)
248	ATLAS <sup>†</sup> 7 TeV 4.6 fb <sup>-1</sup> , W/Z combined cross sec. [16]	34	(80.2)	(2.36)	(4.2)
249	CMS 8 TeV 18.8 fb <sup>-1</sup> W cross sec. and A <sub>ch</sub> [22]	11	10.8(11.0)	0.98(0.99)	0.09(0.1)
250	LHCb 8 TeV 2.0fb <sup>-1</sup> W/Z cross sec. [25]	34	70.2(58.3)	2.07(1.71)	3.5(2.5)
251	ATLAS 8 TeV 20.3 fb <sup>-1</sup> single diff. high-mass cross sec. [58]	12	18.7(?)	1.56(?)	1.3(?)
253	ATLAS 8 TeV 20.3 fb <sup>-1</sup> , Z p <sub>T</sub> cross sec. [27]	27	31.4(29.4)	1.16(1.09)	0.7(0.4)
542	CMS 7 TeV 5 fb <sup>-1</sup> , single incl. jet cross sec., R = 0.7 (extended in y) [59]	158	208.7(204.24)	1.32(1.29)	2.6(2.4)
544	ATLAS 7 TeV 4.5 fb <sup>-1</sup> , single incl. jet cross sec., R = 0.6 [60]	140	204.6(205.2)	1.46(1.47)	3.4(3.5)
545	CMS 8 TeV 19.7 fb <sup>-1</sup> , single incl. jet cross sec., R = 0.7, (extended in y) [61]	185	249.4(229.1)	1.35(1.24)	3.1(2.2)
573	CMS 8 TeV 19.7 fb <sup>-1</sup> , t̄t norm. double-diff. top p <sub>T</sub> & y cross sec. [62]	16	30.4(26.3)	1.90(1.64)	2.1(1.6)
580	ATLAS 8 TeV 20.3 <sup>-1</sup> , t̄t p <sub>T</sub> <sup>2</sup> and m <sub>tℓ</sub> abs. spectrum [63]	15	15.4(20.5)	1.03(1.36)	0.2(1.0)

Data sets employed in the CT18(Z) analysis. The numbers in round brackets are for the CT18Z fit.  $N_{pt,n}$ ,  $\chi^2$  are the number of points and value of  $\chi^2$  for the n-th experiment at the global minimum.  $S_n$  is the effective Gaussian parameter quantifying agreement with each experiment.

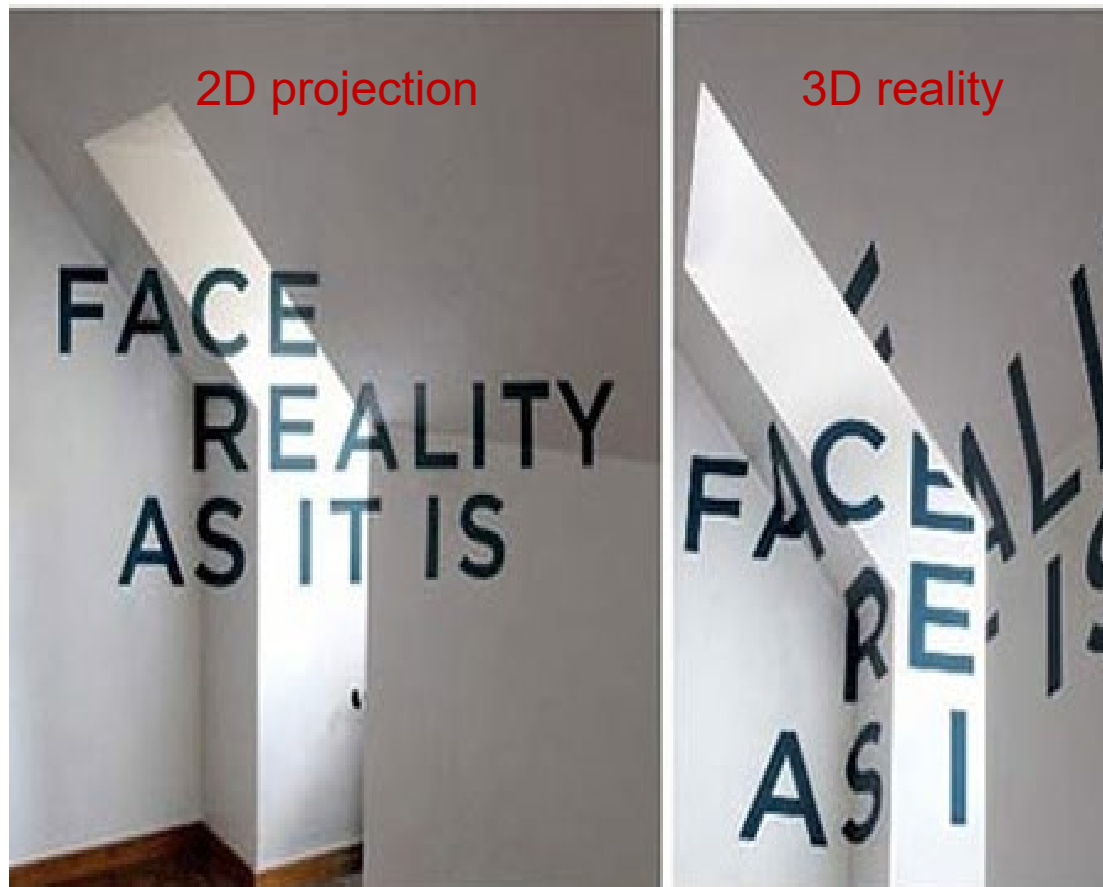
# CT14: parametrization forms

- CT14 relaxes restrictions on several PDF combinations that were enforced in CT10. [These combinations were not constrained by the pre-LHC data.]
  - The assumptions  $\frac{\bar{d}(x, Q_0)}{\bar{u}(x, Q_0)} \rightarrow 1$ ,  $u_v(x, Q_0) \sim d_v(x, Q_0) \propto x^{A_{1v}}$  with  $A_{1v} \approx -\frac{1}{2}$  at  $x < 10^{-3}$  are relaxed once LHC  $W/Z$  data are included
  - CT14 parametrization for  $s(x, Q)$  includes extra parameters
- Candidate CT14 fits have 30-35 free parameters
- In general,  $f_a(x, Q_0) = Ax^{a_1}(1-x)^{a_2}P_a(x)$
- CT10 assumed  $P_a(x) = \exp(a_0 + a_3\sqrt{x} + a_4x + a_5x^2)$ 
  - exponential form conveniently enforces positive definite behavior
  - but power law behaviors from  $a_1$  and  $a_2$  may not dominate
- In CT14,  $P_a(x) = G_a(x)F_a(z)$ , where  $G_a(x)$  is a smooth factor
  - $z = 1 - 1(1 - \sqrt{x})^{a_3}$  preserves desired Regge-like behavior at low  $x$  and high  $x$  (with  $a_3 > 0$ )
- Express  $F_a(z)$  as a linear combination of Bernstein polynomials:

$$z^4, 4z^3(1-z), 6z^2(1-z)^2, 4z(1-z)^3, (1-z)^4$$

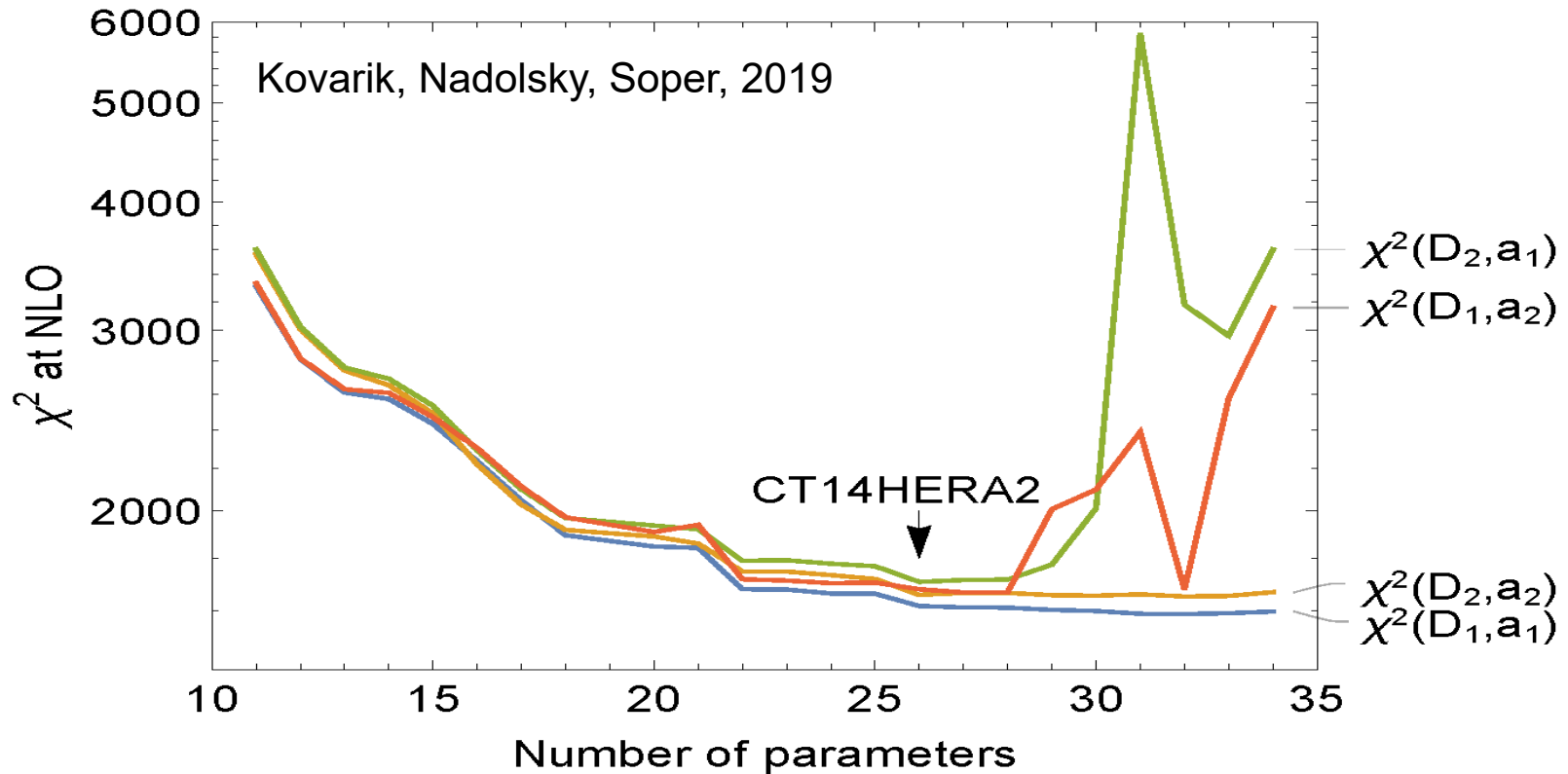
- each basis polynomial has a single peak, with peaks at different values of  $z$ ; reduces correlations among parameters

# If too few parameters



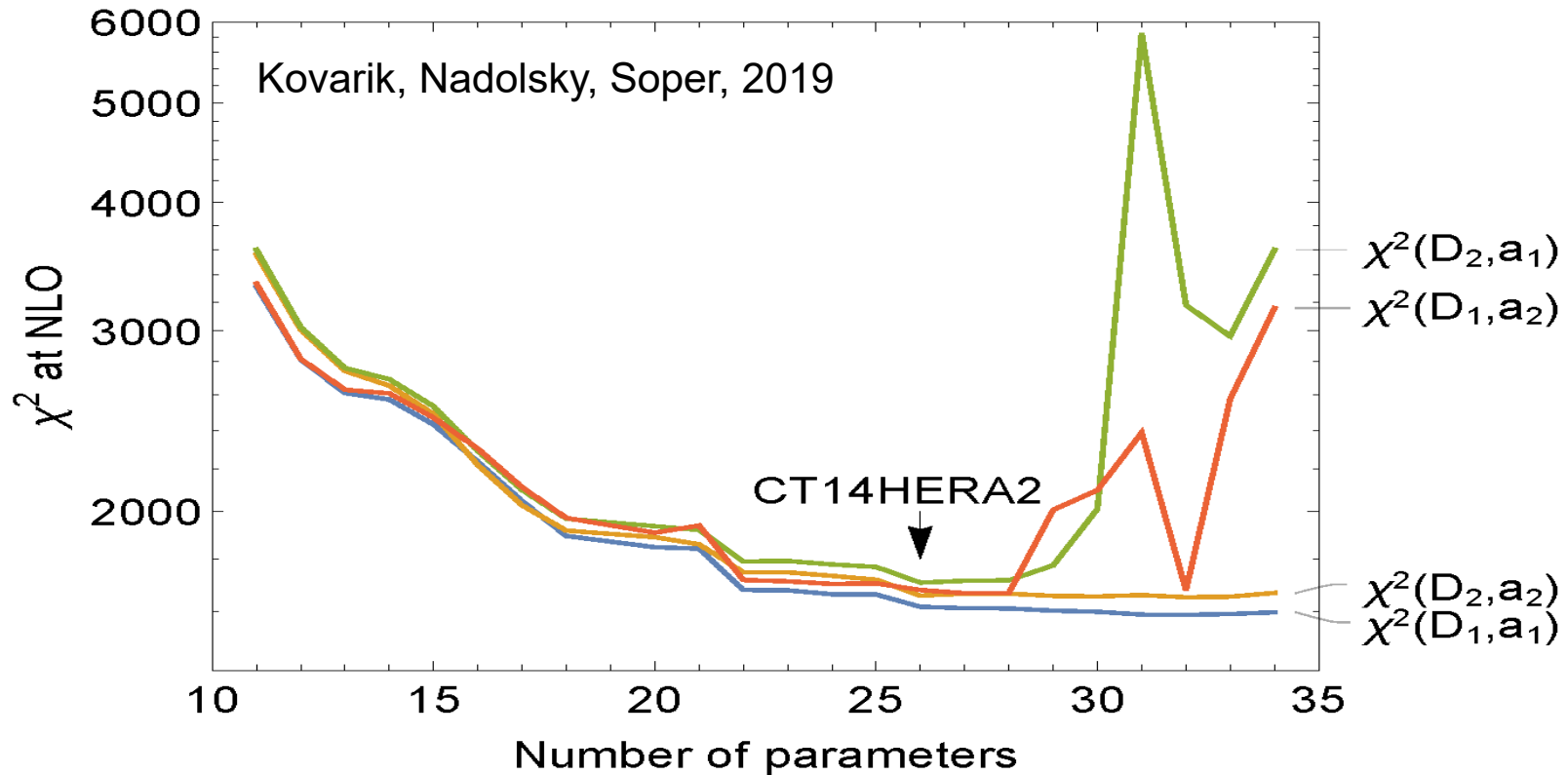
The solution can be consistent and false

# If too many parameters



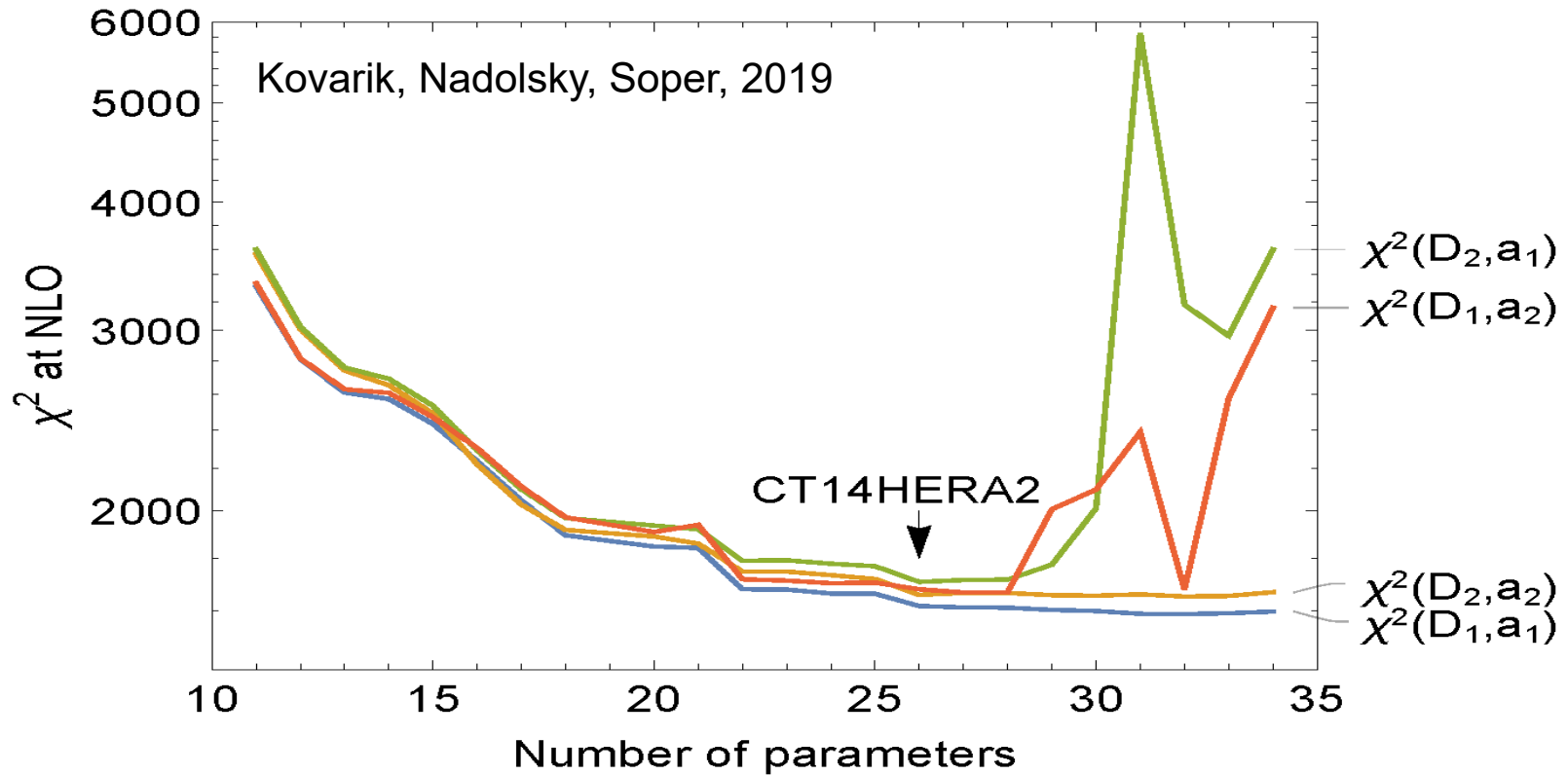
- Randomly split the CT14HERA data set into two halves,  $D_1$  and  $D_2$
- Find parameter vectors  $a_1$  and  $a_2$  from the best fits for  $D_1$  and  $D_2$ , respectively

# If too many parameters



- **Fitted samples:**  $\chi^2(D_1, a_1)$  and  $\chi^2(D_2, a_2)$  uniformly decrease with the number of parameters
- **Control samples:**  $\chi^2(D_2, a_1)$  and  $\chi^2(D_1, a_2)$  fluctuate when the number of parameters is larger than about 30

# If too many parameters



$\approx 30$  parameters (26 in CT14HERA2) is optimal for describing the CT14HERA2 data set



# A shifted residual $r_i$

$r_i(\vec{a}) = \frac{T_i(\vec{a}) - D_i^{sh}(\vec{a})}{s_i}$  are  $N_{pt}$  **shifted residuals** for point  $i$ , PDF parameters  $\vec{a}$

$\bar{\lambda}_\alpha(\vec{a})$  are  $N_\lambda$  **optimized nuisance parameters** (dependent on  $\vec{a}$ )

The  $\chi^2(\vec{a})$  for experiment  $E$  is

$$\chi^2(\vec{a}) = \sum_{i=1}^{N_{pt}} r_i^2(\vec{a}) + \sum_{\alpha=1}^{N_\lambda} \bar{\lambda}_\alpha^2(\vec{a}) \approx \sum_{i=1}^{N_{pt}} r_i^2(\vec{a})$$

$T_i(\vec{a})$  is the theory prediction for PDF parameters  $\vec{a}$

$D_i^{sh}$  is the data value **including the optimal systematic shift**

$$D_i^{sh}(\vec{a}) = D_i - \sum_{\alpha=1}^{N_\lambda} \beta_{i\alpha} \bar{\lambda}_\alpha(\vec{a})$$

$s_i$  is the uncorrelated error

$r_i(\vec{a})$  and  $\bar{\lambda}_\alpha(\vec{a})$   
are tabulated or  
extracted from  
the cov. matrix

# Finding shifted residuals $r_i$ from the covariance matrix

The CTEQ-TEA fit returns tables of  $r_i(\vec{a})$  and  $\bar{\lambda}_\alpha(\vec{a})$  for every  $i$  and  $\alpha$

Alternatively, they can be found from the covariance matrix:

$$r_i(\vec{a}) = s_i \sum_{j=1}^{N_{pt}} (\text{cov}^{-1})_{ij} (T_j(\vec{a}) - D_j), \quad \bar{\lambda}_\alpha(\vec{a}) = \sum_{i,j=1}^{N_{pt}} (\text{cov}^{-1})_{ij} \frac{\beta_{i\alpha}}{s_i} \frac{(T_j(\vec{a}) - D_j)}{s_j}$$

# Vectors of data residuals

For every data point  $i$ , construct a vector of residuals  $r_i(\vec{a}_k^\pm)$  for 2N Hessian eigenvectors.  $k = 1, \dots, N$ , with  $N = 28$  for CT14 NNLO:

$$\vec{\delta}_i = \{\delta_{i,1}^+, \delta_{i,1}^-, \dots, \delta_{i,N}^+, \delta_{i,N}^-\} \quad [N = 28]$$

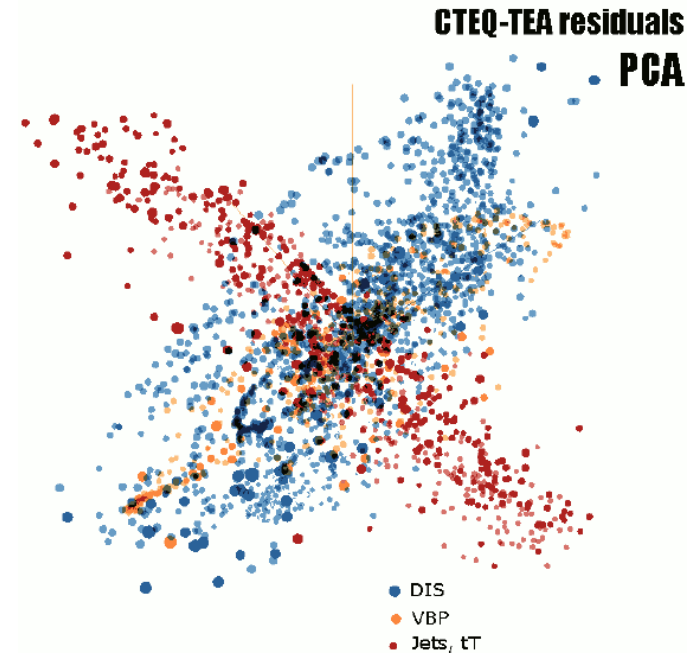
$$\delta_{i,k}^\pm \equiv \left( r_i(\vec{a}_k^\pm) - r_i(\vec{a}_0) \right) / \langle r_0 \rangle_E$$

-- a 56-dim vector normalized to  $\langle r_0 \rangle_E$ , the root-mean-squared residual for the experiment  $E$  for the central fit  $\vec{a}_0$

$$\langle r_0 \rangle_E \equiv \sqrt{\frac{1}{N_{pt}} \sum_{i=1}^{N_{pt}} r_i^2(\vec{a}_0)} \approx \sqrt{\frac{\chi_E^2(\vec{a}_0)}{N_{pt}}}$$

$\langle r_0 \rangle_E \approx 1$  in a good fit to  $E$

$r_i$  is defined in the backup



The TensorFlow Embedding Projector (<http://projector.tensorflow.org>) represents CT14HERA2  $\vec{\delta}_i$  vectors by their 10 principal components indicated by scatter points. A sample 3-dim. projection of the 56-dim. manifold is shown above. A symmetric 28-dim. representation can be alternatively used.

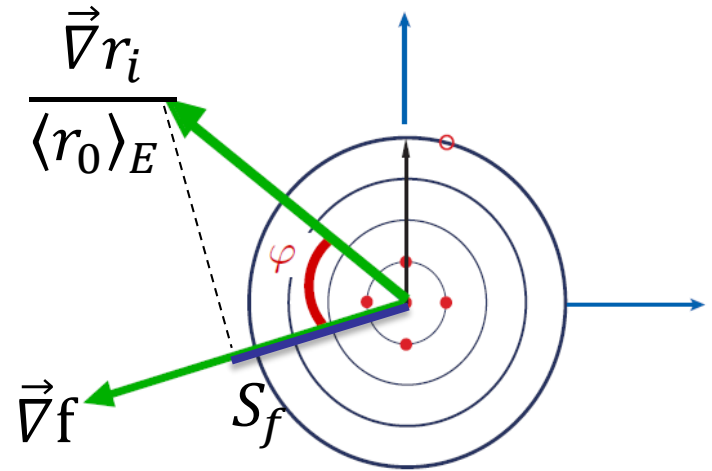
# Correlation $C_f$ and sensitivity $S_f$

The relation of data point  $i$  on the PDF dependence of  $f$  can be estimated by:

- $C_f \equiv \text{Corr}[\rho_i(\vec{a}), f(\vec{a})] = \cos\varphi$

$\vec{\rho}_i \equiv \vec{\nabla} r_i / \langle r_0 \rangle_E$  -- gradient of  $r_i$  normalized to the r.m.s. average residual in expt E;

$$(\vec{\nabla} r_i)_k = (r_i(\vec{a}_k^+) - r_i(\vec{a}_k^-)) / 2$$



$C_f$  is **independent** of the experimental and PDF uncertainties. In the figures, take  $|C_f| \gtrsim 0.7$  to indicate a large correlation.

- $S_f \equiv |\vec{\rho}_i| \cos\varphi = C_f \frac{\Delta r_i}{\langle r_0 \rangle_E}$  -- projection of  $\vec{\rho}_i(\vec{a})$  on  $\vec{\nabla} f$

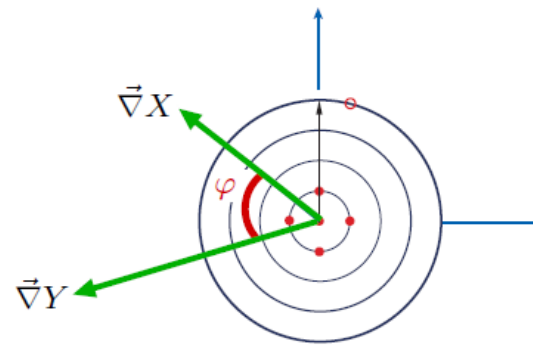
$S_f$  is proportional to  $\cos\varphi$  and the ratio of the PDF uncertainty to the experimental uncertainty. We can sum  $|S_f|$ .

In the figures, take  $|S_f| > 0.25$  to be significant.

# $L_2$ sensitivity, definition

## Tolerance hypersphere in the PDF space

2-dim (i,j) rendition of N-dim (22) PDF parameter space



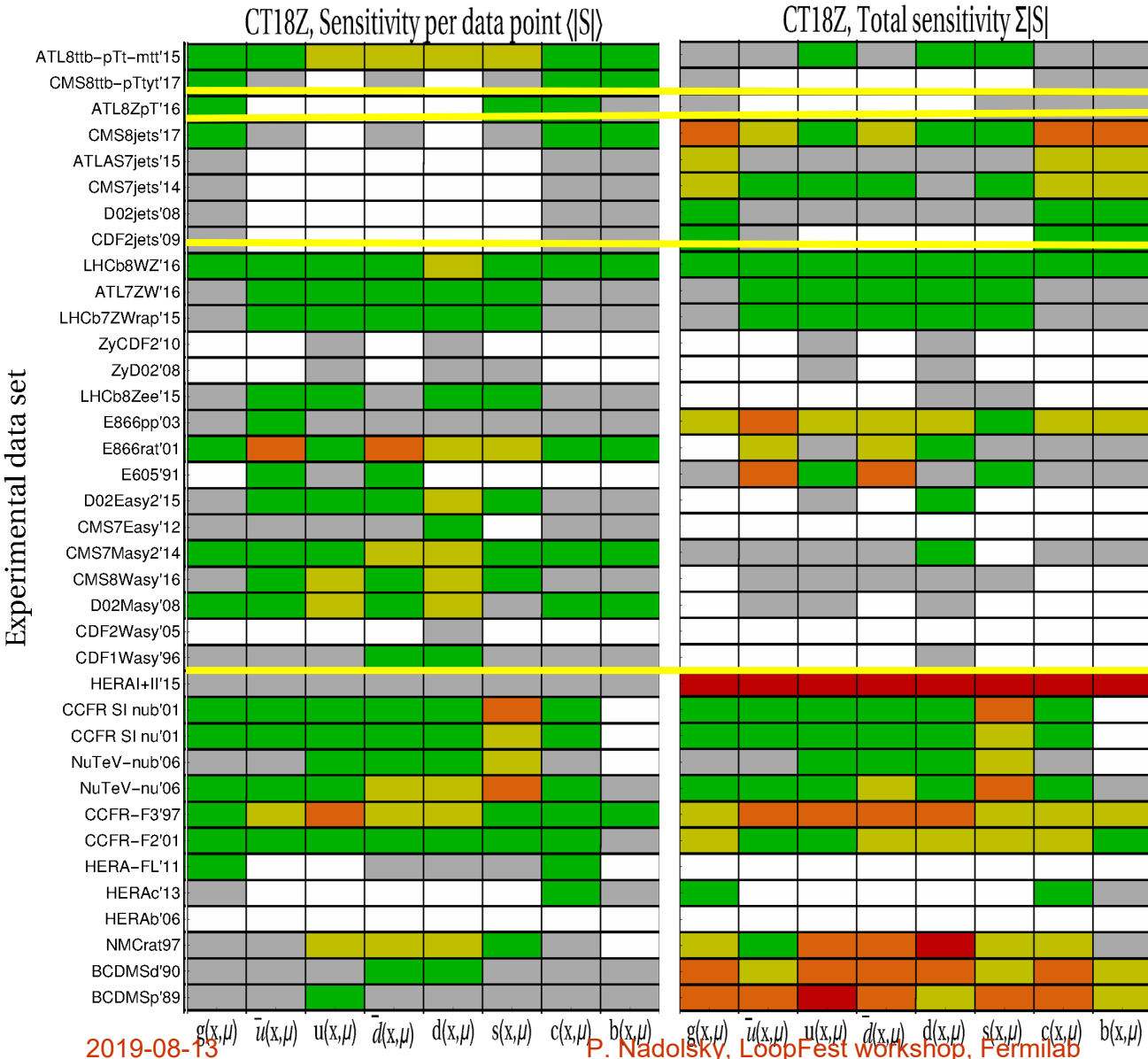
(b)  
Orthonormal eigenvector basis

$L_2$  sensitivity. Take  $X = f_a(x_i, Q_i)$  or  $\sigma(f)$ ;  $Y = \chi_E^2$  for experiment  $E$ . Find  $\Delta Y(\vec{z}_{m,X})$  for the displacement  $|\vec{z}_{m,X}| = 1$  along the direction  $\vec{\nabla}X / |\vec{\nabla}X|$  (corresponding to  $\Delta\chi_{tot}^2 = T^2$  and  $X(\vec{z}) = X(0) + \Delta X$ ):

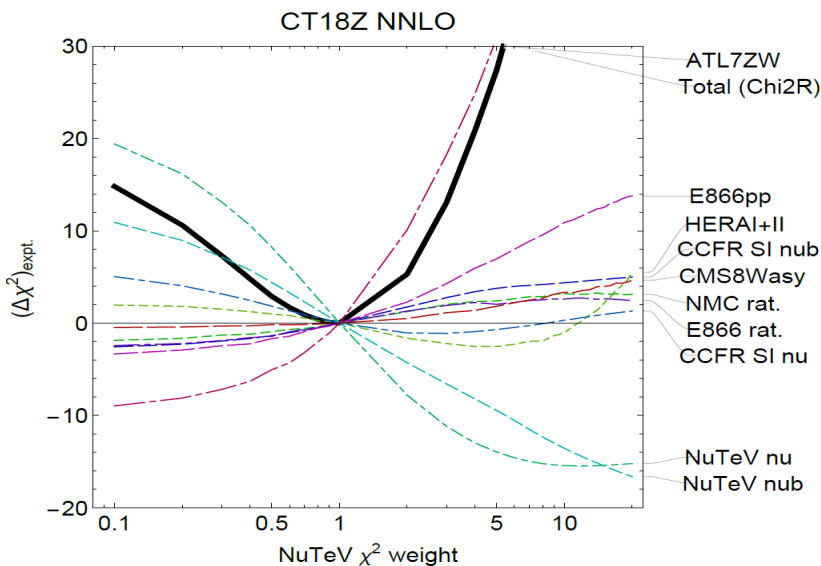
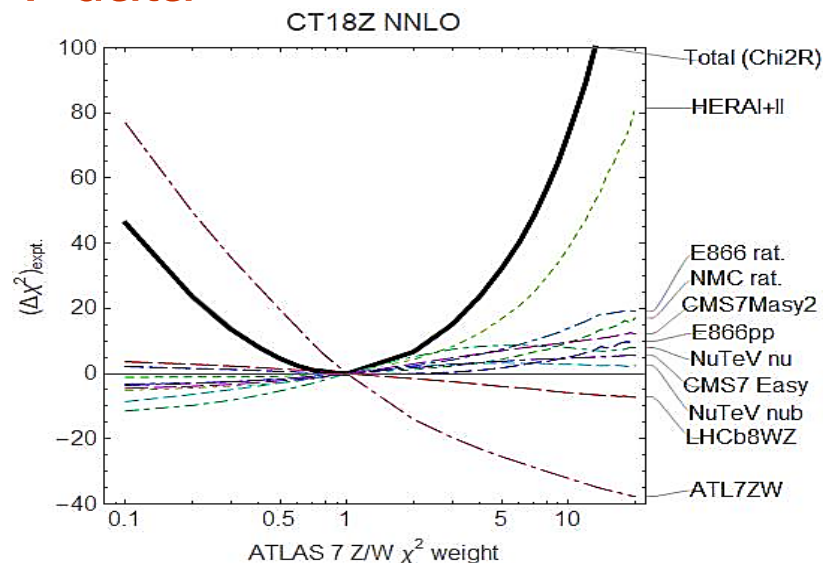
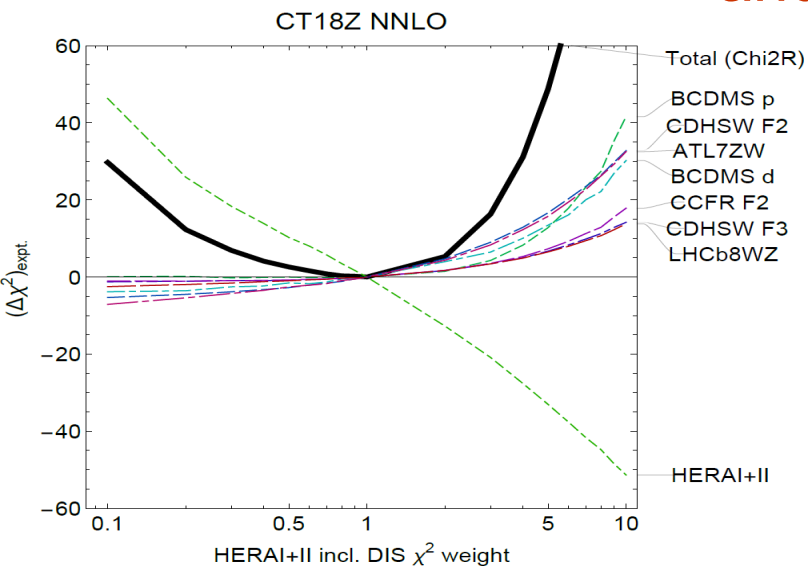
$$S_{f,L_2} \equiv \Delta Y(\vec{z}_{m,X}) = \vec{\nabla}Y \cdot \vec{z}_{m,X} = \vec{\nabla}Y \cdot \frac{\vec{\nabla}X}{|\vec{\nabla}X|} = \Delta Y \cos \varphi$$

# Sensitivity of hadronic experiments to PDFs

**For the CT18Z NNLO data set**



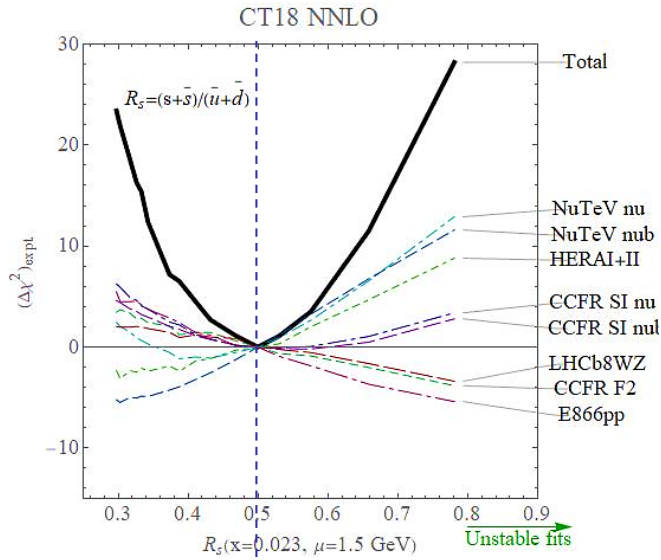
# LM scans on $\chi^2$ weights of HERA I+II, ATLAS 7 Z/W, and NuTeV data



Fits with varied weights and LM scans reveal a disagreement between important DIS [primarily HERA, CCFR, NuTeV,...] and DY [primarily ATL7ZW, E866, LHCb8WZ,...] experiments. This is more pronounced for large- $x$  gluon as well as strangeness.

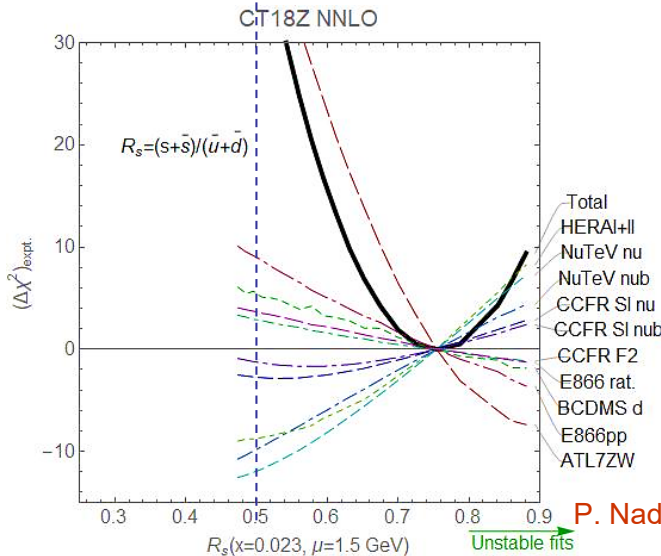


# Lagrange Multiplier scan: $R_s(x = 0.023, \mu = 1.5 \text{ GeV})$

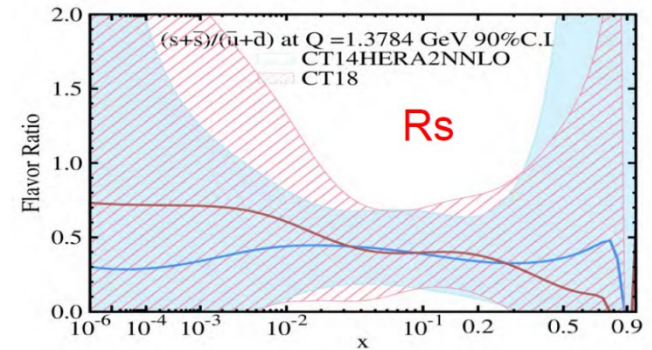


The CT18Z strangeness is increased primarily as a result of including the ATLAS 7 TeV W/Z production data (not in CT18), as well as because of using the DIS saturation scale and  $m_c^{\text{pole}} = 1.4 \text{ GeV}$

In either CT18 or CT18Z fit, observe instability in the fits for  $R_s > 1$  at  $x = 0.01 - 0.1$

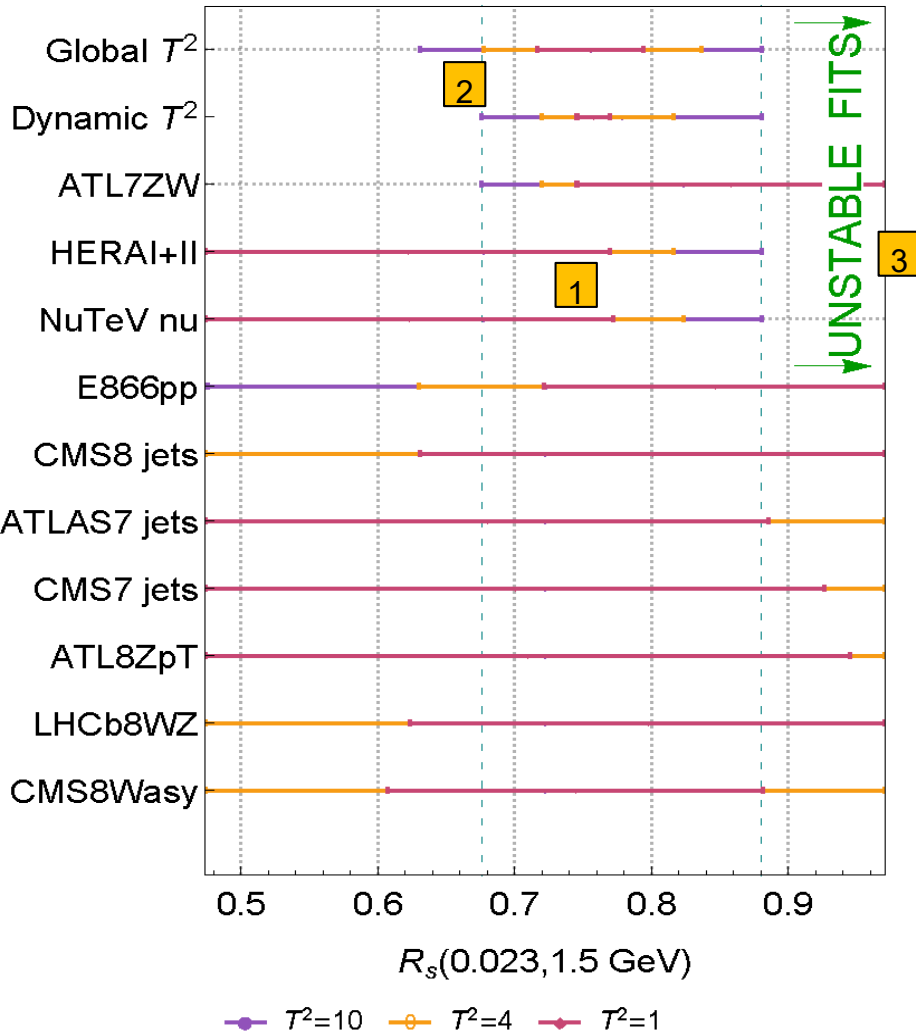


Compare to



# Effect on PDF uncertainties

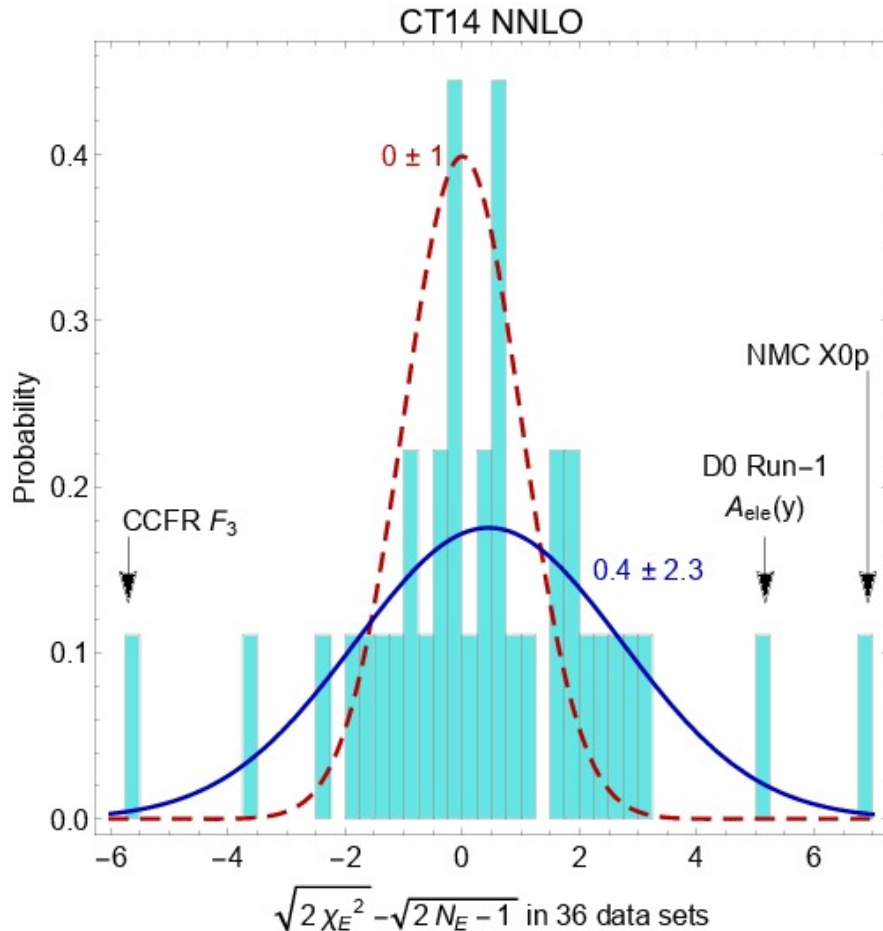
CT18Z NNLO uncertainties



The LM scan reveals details not captured by other methods

- 1 **Nonlinearities:** the error bands for tolerance  $T^2 = 1, 4, 10$  may not scale according to the Gaussian distribution
- 2 **Tensions:** in the affected direction(s), the global tolerance and **especially dynamic tolerance** may underestimate the true PDF error.
- 3  **$\chi^2$  instability:** Neither the “global  $T^2$ ” nor “dynamic  $T^2$ ” reflect instability of fits at  $R_s > 0.9$

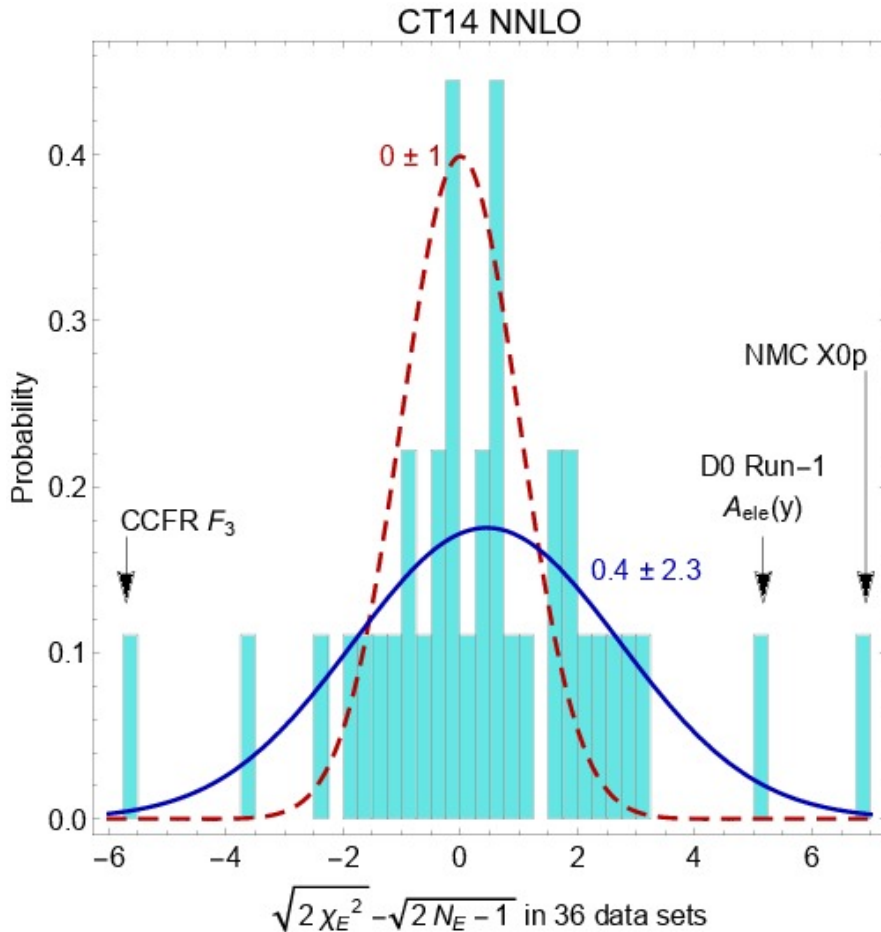
# Effective Gaussian variables



Define  $S_n(\chi^2, N_{pt})$  for experiment  $n$  so that, in a perfect fit, it would approximately obey the standard normal distribution  $N(0,1)$  (mean=0, half-width=1) independently of  $N_{pt,n}$

[H.-L. Lai et al., arXiv:1007.2241;  
S.Dulat et al., arXiv:1309.0025;  
K. Kovarik, P.N., D. Soper,  
arXiv:1905.06957]

# Effective Gaussian variables



$$S_n(\chi^2, N_{pt}) \equiv \sqrt{2\chi^2} - \sqrt{2N_{pt} - 1}$$

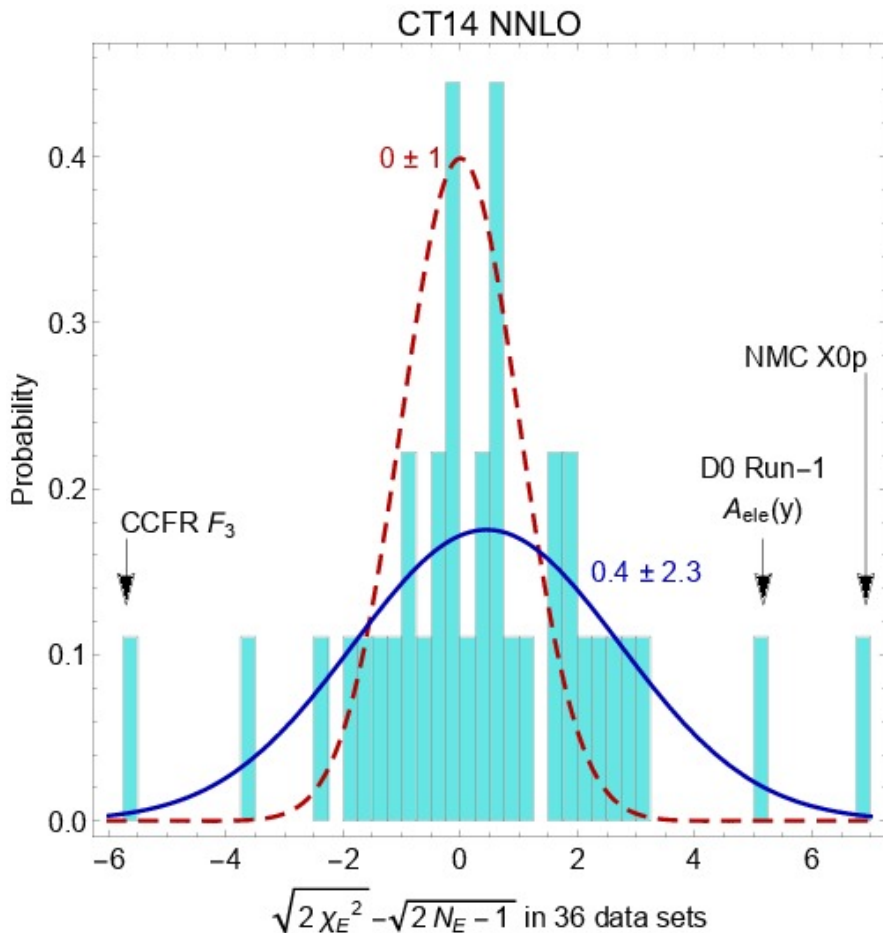
$S_n(\chi_n^2, N_{pt,n})$  are Gaussian distributed with mean 0 and variance 1 for  $N_{pt,n} \geq 10$

**[R.A.Fisher, 1925]**

Even more accurate  $(\chi^2, N_{pt})$ :  
**T.Lewis, 1988**

An empirical  $S_n$  distribution can be compared to  $N(0,1)$  visually or using a statistical (Anderson-Darling, Kolmogorov-Smirnov, ...) test

# Effective Gaussian variables



Some  $S_n$  are too big or too small in a global fit

## CT14 NNLO:

- $S_n > 4$  for NMC DIS  $ep$  cross section and D0 Run-1 electron charge asymmetry
- These data sets are eliminated in CT14HERA2/CT18 fits
- The rest of CT14 experiments are reasonably consistent;  $S_n \sim N(0.3, 1.6)$
- Qualitatively similar  $S_n$  distributions for MMHT, NNPDF3.X

# Effective Gaussian variables

